Mechanochemical Synthesis of Pharmaceutical Cocrystal Suspensions via Hot Melt Extrusion: Feasibility Studies and Physicochemical Characterisation

Li, S., Yu, T., Tian, Y., McCoy, C. P., Jones, D. S., & Andrews, G. P. (2016). Mechanochemical Synthesis of Pharmaceutical Cocrystal Suspensions via Hot Melt Extrusion: Feasibility Studies and Physicochemical Characterisation. *Molecular Pharmaceutics*, *13*(9), 3054–3068. https://doi.org/10.1021/acs.molpharmaceut.6b00134

Published in:
Molecular Pharmaceutics

Document Version:
Peer reviewed version

Mechanochemical Synthesis of Pharmaceutical Cocrystal Suspensions via Hot Melt Extrusion: Feasibility Studies and Physicochemical Characterisation

Shu Li, Tao Yu, Yiwei Tian, Colin P. McCoy, David S. Jones and Gavin P. Andrews*,
Pharmaceutical Engineering Group, School of Pharmacy, Medical Biology Centre,
Queen's University, Belfast BT9, Northern Ireland

Correspondence to: Gavin P. Andrews (Telephone: +44-2890-97-2646; E-mail: g.andrews@qub.ac.uk)

Running Title: Cocrystals via Mechanochemistry

Abstract:

Engineered Cocrystals offer an alternative solid drug form with tailored physicochemical properties. Interestingly, although cocrystals provide many new possibilities they also present new challenges, particularly in regard to their design and large-scale manufacture. Current literature has primarily focused on the preparation and characterization of novel cocrystals typically containing only the drug and coformer, leaving the subsequent formulation less explored. In this paper we propose, for the first time, the use of hot melt extrusion for the mechanochemical synthesis of pharmaceutical cocrystals in the presence of a meltable binder. In this approach, we examine excipients that are amenable to hot melt extrusion, forming a suspension of cocrystal particulates embedded in a pharmaceutical matrix. Using ibuprofen and isonicotinamide as a model cocrystal reagent pair, formulations extruded with a small molecular matrix carrier (xylitol) were examined to be intimate mixtures wherein the newly formed cocrystal particulates were physically suspended in a matrix. With respect to formulations extruded using polymeric carriers (Soluplus® and Eudragit® EPO, respectively), however, there was no evidence within PXRD patterns of either crystalline ibuprofen or the cocrystal. Importantly, it was established in this study that an appropriate carrier for a cocrystal reagent pair during HME processing should satisfy certain criteria including limited interaction with parent reagents and cocrystal product, processing temperature sufficiently lower than the onset of cocrystal T_m, low melt viscosity and rapid solidification upon cooling.

Introduction

Pharmaceutical material science is fundamental in the design and development of new and improved drug delivery platforms. In particular, crystal engineering has brought the possibility of designing new drug complexes (cocrystals) that provide an opportunity to modify the properties of the parent drug. Possible improvements include solid-state properties, aqueous solubility, dissolution rate and bioavailability[1–3], the latter being particularly important for BCS Class II drugs. Undoubtedly, over the last decade, the use of crystal engineering to optimise the physical properties of drugs has gained significant attention[4,5]. This may be attributed to the fact that the effective delivery of drugs to a patient in a safe and cost-effective manner is significantly influenced by the physicochemical properties of drug in the solid state. Moreover, cocrystals manufactured via crystal engineering offer an alternative solid drug form with tailored physicochemical properties and represent a significant opportunity to generate intellectual property. Interestingly, although cocrystals provide many new possibilities they also present new challenges, particularly in regard to their design and large-scale manufacture.

Pharmaceutical cocrystals are multi-component molecular complexes consisting of a drug and a cocrystal former (coformer) in a well-defined stoichiometry, formed mainly via hydrogen bonding, halogen bonds and/or π−π stacking supramolecular interactions[4–6]. The wide range of coformer properties and interactions in solid and solution phase (depending upon manufacturing method) provides an opportunity to alter physicochemical properties. It has been previously reported that successful cocrystallization requires complimentary functional groups on drug and coformer, typical examples including carboxylic acids and amides[7].

Cocrystals are traditionally manufactured using traditional solvent evaporation[8,9]. However, more recently there has been a strong and increasing demand for clean and environmentally friendly processes that focus on green methods of conducting chemical reactions in the absence of solvents. Of particular relevance within the pharmaceutical arena has been the recent interest in, and success of, grinding methods, for pharmaceutical cocrystallisation via mechanochemical reactions[10–13]. This has been driven by the

fact that pharmaceutical cocrystal synthesis is largely due to the formation of supramolecular interactions that can be broken and reformed under mild mechanical conditions.

Dry/neat grinding, are simple and commonly used processes for mechanochemical synthesis within solid blends[14]. These techniques have emerged as a useful, alternative technique to the traditional solvent-intensive methods for pharmaceutical cocrystal synthesis and production. However, there has been a number of reports presenting incomplete cocrystallisation using dry grinding[15]. Liquid-assisted grinding has, therefore, gained considerable favour because of the possibility of providing dramatically improved productivity via the addition of only small amounts of liquid to a typical grinding process[16–24]. It is, however, occasionally criticised for the unintentional production of cocrystal solvates[25]. In addition, the role of the added liquid differs from case to case, resulting in difficulties in clarifying reaction mechanisms[16,20,26]. More recently, another advanced solvent-free continuous manufacturing method, hot-melt extrusion (HME), has also emerged as an, easy to scale, alternative for mechanochemical cocrystal synthesis[27–31]. Interestingly, current literature has primarily focused on the preparation and characterization of novel cocrystals typically containing only the drug and coformer, leaving the subsequent formulation less explored[32]. IN this regard, Etter *et al (1993)* reported cocrystallisation in the presence of a third component by solid-state grinding[33]. The resulting product contained cocrystals of the complementary reagent pair, as well as the additional inert component that remained unchanged following cocrystal manufacture. Furthermore, cocrystals formed in the presence of the inert component had the same crystal structure as cocrystals grown from solution. More recently, driven by polymer-induced heteronucleation studies[34], it has also been shown that the involvement of macromolecules in the cocrystal pool may also catalyse the reaction during mechanochemical preparation of cocrystals[35]. The cocrystals manufactured using polymer-assisted grinding methods were shown to negate the risk of generating undesirable solvates, while providing excellent control over the particle size of the resultant cocrsytals. Moreover, other important work has investigated cocrystal manufacture in the presence of an inert excipient[36]. The effects of coformers on phase

transformation and release profiles of carbamazepine (CBZ) cocrystals in hydroxypropyl methylcellulose (HPMC) matrix tablets were examined. It was shown that HPMC partially inhibited the crystallisation of CBZ during dissolution.

If mechanochemical synthesis is to deliver its promise of being a clean manufacturing technology, it must be shown to be capable of operating in an environment devoid of solvent and be scalable. Furthermore, it is well recognised that cocrystal synthesis is only one step in the development of suitable oral dose formulations with other components (e.g., lubricant, glidant, diluent) and unit operations (milling, sieving, blending, compression, filling) being required before a successful drug product is produced. In light of the above, we propose, for the first time, the use of hot melt extrusion, a solventless, continuous and easily scalable technique, for the mechanochemical synthesis of pharmaceutical cocrystals in the presence of a meltable binder. In this approach, we examine chemically inert excipients that are amenable to hot melt extrusion, forming a suspension of cocrystal particulates embedded in a pharmaceutical matrix. We aim to understand if inert meltable carriers can be used to facilitate the production of a solid extrudate while also acting as a catalyst for cocrystallisation during melt-extrusion processing.

Selection of Formulation Components

Cocrystal Reagents

Ibuprofen (Ibu, Figure 1a) is a BCS Class II drug[37] and has dissolution limited absorption, particularly in acidic environment. Ibu has been widely used as a cocrystal reagent, principally because it is inexpensive and contains a carboxylic acid functional group that makes it an excellent donor to form intermolecular hydrogen bonds with cocrystal reagents that possess a lone pair of electrons[38].

Isonicotinamide (IsoNA, Figure 1a), although not classified as a GRAS substance, has been shown to be an effective coformer with many literature examples of carboxylic acid-IsoNA cocrystals[39–41].

Matrix Excipients

Recently it has been demonstrated that a small molecular weight sugar alcohol, mannitol, could be used as a matrix platform capable of significantly increasing

the dissolution rate of poorly water soluble drugs[42]. In the work reported by Thommes et al., (2011) HME was used to manufacture a suspension of crystalline drug in a molten excipient to produce a uniform distribution of fine particles. Rapid crystallization of mannitol 'fixed' the suspended drug particles producing a solid homogeneous extrudate. In the work described in this article, we adapt the concept of extruded crystalline suspensions and apply the aforementioned preliminary criteria into matrix carrier selection. However, due to thermal stability considerations, mannitol, which melts at 160°C, was not used. Consequently, xylitol which melts at a significantly lower temperature was employed.

Despite the advantages sugar alcohols offer with respect to low melt viscosity and rapid solidification, extrudates may be difficult to shape post extrusion owing to the rigidity of their crystalline structure. Thus, the use of thermoplastic polymers was also examined. Eudragit® E PO and Soluplus® were chosen for such purposes owing to their relatively low T_g and hence wider processing window. If cocrystals can be successfully manufactured and precipitated from an amorphous polymeric carrier, an amorphous suspension also referred to as a glass suspension could be formulated.

Materials & Methodology

Materials

Ibuprofen, isonicotinamide, and xylitol were purchased from Sigma-Aldrich (St. Louis, MO, USA). Eudragit®E PO was obtained from Evonik (Essen, Germany). Soluplus® was kindly supplied by BASF Corporation (Ludwigshafen, Germany). All other chemical reagents used were of analytical grade.

Differential Scanning Calorimetry (DSC)

Cocrystallisation feasibility studies and extrudate analyses were conducted on a DSC 4000 (heat flux single furnace), and a DSC 8000 (power compensation dual furnace), respectively (Perkin-Elmer, Windsor, Berkshire, UK). Both instruments were calibrated at the respective ramp rates with indium and zinc for both melting point and heat of fusion. Either dry nitrogen or helium was purged at a flow rate of 40mL/min through the sample and reference cells to maintain an

inert atmosphere. 3-5mg of sample was accurately weighed into an aluminium pan and crimped using an aluminium pan lid. The crimped pan set was then subjected to a thermal ramp at 20°C/min in DSC 4000, and 200°C/min in DSC 8000, respectively, from -60°C to 200°C. The polymeric candidates were subjected to modulated DSC (TA Q100, TA Instruments) at 2°C/min, with an amplitude and frequency of ±0.6°C every 40s to enable the determination of the glass transition temperature (T_g).

Thermogravimetric Analysis (TGA)

The decomposition temperature for each individual substance was determined using a Thermal Advantage Model Q500 TGA (TA instruments, Leatherhead, UK). Ramp tests were performed on powdered samples (5-10 mg) heated at 10°C/min over a range from 0°C to 400°C. Dry nitrogen (flow rate sample: 60 mL/min, flow rate balance: 40 mL/min) was purged through the sample chamber during all experiments to maintain an inert environment and hence prevent oxidation. The temperature at which a 5% weight loss occurred was recorded for each sample and considered as the onset of material decomposition.

Preparation of the Reference Cocrystal Standard

0.01 moles of equimolar ibuprofen-isonicotinamide mixture was dissolved in 50mL methanol and stirred at room temperature until complete dissolution was achieved. The resulting clear solution was left in a fume hood covered with a funnel to allow slow evaporation of the solvent for 48 hours. The precipitate was collected and subsequently stored in an oven at 45°C for a further 24 hours to remove any residual solvent. The resulting material was gently pulverized using a mortar and pestle, sized through a 220µm sieve and stored in a vacuum desiccator before being subjected to further analysis.

Cocrystallisation via Ball-Milling

Equimolar ibuprofen-isonicotinamide mixtures with or devoid of excipient were ground using a ball mill (MM200, Retsch, Reinische, Haan, Germany) at a frequency of 20 s^{-1} frequency for pre-determined periods of time (i.e. 2, 5, 8, 15,

30, 45 and 60 minutes). The resulting pulverized mixtures were sized through a 220μm sieve before being subjected to further characterisation.

Cocrystallisation via Hot-Melt Extrusion

Physically mixed blends of each formulation were manually fed into a co-rotating twin-screw HAAKE Mini-lab Extruder (HAAKE Minilab, Thermo Electron Corporation, Stone, Staffordshire, UK). The process temperature was determined according to the melting temperature(s) of the crystalline compound(s) in the physical blend with screw speed set at 10rpm. For the formulations containing xylitol, the HME parameters were slightly modified to prevent early-stage phase separation and late-stage die blockage. In particular, the processing was divided into two stages: the 'feeding stage' where temperature was set at the melting point of the polyol and screw speed set at 10rpm; and the 'flushing stage' where temperature was set 7°C lower than the polyol melting temperature and screw speed set at 50rpm (Table 1). All collected products were pulverized by mortar and pestle and subsequently stored in a desiccator over silica gel at room temperature prior to further analyses.

Powder X-ray Diffraction (PXRD)

Samples were analysed at room temperature using a MiniFlex II Desktop Powder X-ray Diffractometer (Rigaku Corporation, Kent, England) equipped with Cu Kβ radiation, at a voltage of 30 kV and a current of 15 mA. The powdered samples were gently consolidated on a glass top-loading sample holder with 0.2mm depression. All samples were scanned within the angular range of 1.5-40° 2θ in continuous mode with a sampling width of 0.03° and a scan speed of 2.0°/min.

Quantification of Cocrystal Yielding

The peak area of the cocrystal characteristic peak at 3.3° 2θ for each sample was used to determine the cocrystal yield[43]. A series of physical mixtures containing the reference cocrystal and xylitol at 10 different cocrystal loadings, 10, 20, 30, 40, 50, 60, 70, 80, 90 & 100% w/w, respectively, were prepared through gentle mixing. The blended samples were placed into a 0.2mm-deep squared indentation on the glass sample holder for PXRD analysis. The integration region

was set between [2.400~4.050° 2θ] with manual background subtraction using the IntegralAnalysis Version 6.0 (Rigaku Corporation, Kent, England). A calibration curve, y=284.877x-668.959 (R^2=0.998) was constructed using linear regression of the average peak area against theoretical cocrystal concentration in the blends. The calibration curve was validated for linearity, accuracy, precision, LoD and LoQ according to the methods recommended in the ICH guidelines[44] (data included as supporting documents).

FT Infrared Spectroscopy (FTIR)

FT-IR spectroscopy was used to investigate molecular interactions and to identify the structure of Ibu/IsoNA cocrystal. Experiments were performed using a Fourier transform infrared spectrophotometer model 4100 (FT/IR-4100) (Jasco, Easton, MD), incorporated with the Version 2 Jasco Spectra Manager Software. A scanning range of 4000-400cm^{-1} with 4.0cm^{-1} resolution and 16 scans per spectrum was used for all samples. Prior to FTIR spectroscopic analysis, samples were gently ground with dry potassium bromide (KBr) powder using an agate mortar and pestle and compressed at approximately 7.5Pa for 60s to prepare a KBr disk. The concentration of the samples in a KBr disk was maintained at 0.67% (2mg sample plus 298mg KBr) for all analyses.

Raman Microscopy & Mapping

Raman spectroscopic analyses were conducted using a RamanMicro 300 Raman microscope (Perkin Elmer, Windsor, Berkshire, UK) coupled with an Avalon Raman station R3 Model AVRS003A spectrometer (Avalon Instruments, Belfast, UK). A magnification of 20x with a total exposure time of 20s (4s acquisition × 5) was used for all samples. Data was collected from 200-3200cm^{-1} and analysed using Spectrum v6.3.4 software with an automatic baseline correction. Cross sections of rod shaped extrudates were mapped with a 50μm spacing between each sampling point. Approximately 4000 points were collected across the exposed mapping area for the cross section of one pellet. The laser power was set at 80% throughout the mapping process to avoid sample saturation. Spectrum IMAGE R1.6.4.0394 software was used to conduct mapping analysis for each examined sample. The characteristic peak associated with the

Ibu/IsoNA cocrystal at 1020 cm^{-1} was used in the single wavenumber mode. The maps were shown with an ordinate axis range of [1000-7500 INT], whilst the horizontal X axis range and the vertical Y axis range were both 0-2350 μm. A rainbow cubic look-up table was utilized to illustrate the intensity of the chosen cocrystal peak.

Polarized Light Microscope (PLM)

A polarized light microscope (Olympus BX50F4, Microscope Service and Sales, Surrey, UK*)* was used to study the morphology of the melt-extruded cocrystals in comparison to that of the unprocessed ibuprofen. Polarized light micrographs of each sample were captured at room temperature using a Pixelink Megapixel Firewire Camera and Pixelink software (Scorpion Vision Ltd., Lymington, UK). The milled sample within the size range 180~212μm was dispersed in a drop of mineral oil on a glass slide. All measurements were performed at a magnification of 200x with the polariser and analyser positioned perpendicularly.

In-vitro Dissolution Study

In-vitro drug dissolution tests were conducted to evaluate solubility enhancement and dissolution behaviour of the melt extruded Ibu/IsoNA cocrystals in comparison with that of the unprocessed ibuprofen. Release studies were performed using a Caleva dissolution tester 10ST (GB Caleva Ltd., Dorset, UK) according to the BP 2011 apparatus II, paddle method. The powdered samples were sieved to the same particle size [180~212μm] prior to testing. Each formulation, containing equivalent to 120mg Ibu, was tested in 600mL deionized water at 37±0.5°C using a paddle rotation speed of 75rpm. 3mL aliquots were withdrawn from each dissolution vessel at regular time intervals and filtered through a 0.45μm Millipore filter unit (MILLEX®-GS, Millipore, Carrigtwohill Co, Cork, Ireland) before being subjected to a validated HPLC analysis. Immediately after sample withdrawal, 3mL of blank dissolution media was added into each vessel to maintain the overall media volume.

High Performance Liquid Chromatography (HPLC)

The concentration of ibuprofen in each sampled aliquot was determined using HPLC analysis. The HPLC system consisted of a Waters binary HPLC pump 1525, a Plus Auto sampler 717, an In-line Degasser AF and a Dual λ Absorbance Detector 2487 (Waters, Massachusetts, USA). Sampled aliquots were analysed at 220 nm using a Jupiter C18 300 column (5μm) with a length of 250 mm and a diameter of 4.60 mm (Phenomenex, Macclesfield, UK). The mobile phase consisted of 85% methanol and 15% deionized water containing 0.2% TFA. The flow rate was set at 1 mL/min and the column chamber was maintained at 40°C for the entire analytical procedure. The average retention times under these conditions were 4.56 minutes for Ibu, 3.40 minutes for IsoNA, while other components were tested to show no interference. When Soluplus® was involved, the mobile phase was changed to a 70:30 ratio between the organic and inorganic solutions with a retention time of 8.76 minutes for ibuprofen to avoid interference. Peak areas were calculated using Breeze 3.30 software. Standard solutions were prepared in triplicate using methanol and deionized water at 1:1 volume ratio for the generation of a linear calibration curve (R^2>0.999). The calculated concentrations of ibuprofen dissolved during the dissolution test were then plotted as a function of time.

Storage Stability

The extruded suspensions were stored either in a desiccator over silica gel for 12 months under ambient conditions or in a desiccator over saturated sodium chloride solution at 20°C and 70%RH for 12 months. The aged suspensions were examined by PXRD and the cocrystal content in each formulation was calculated using the aforementioned yielding quantification.

Statistical Analysis

Statistical analyses were conducted using a one-way analysis of variance (GraphPad Prism 6.0). Individual differences between treatment groups were identified using Tukey's *post-hoc* test with $P<0.05$ denoting statistical significance.

Results

Formation of Ibu/IsoNA Cocrystal

In this work we considered that Ibu and IsoNA would form a cocrystal at an equimolar stoichiometric ratio[45–48]. This would be facilitated by the interaction of the carboxylic acid functional group of Ibu, the IsoNA amide and the N on the pyridine of IsoNA[26]. With respect to IBu and IsoNA, the carboxylic acid group, would be highly pertinent in successful formation of cocrystal with carboxylic acid-aromatic nitrogen and carboxylic acid-amide synthons being the major interactions present (Figure 1b).

Prior to addition of pharmaceutical excipients and evaluation of extrusion as a continuous process for mechanochemical synthesis of cocrystals, we employed ball milling to determine the feasibility of forming a cocrystal product from an Ibu/IsoNA blend at a 1:1 molar ratio. Conventional DSC analysis at a heating rate of 20°C/min was used to confirm the formation of the Ibu/IsoNA cocrystal. It has been previously reported in many articles that the melting temperature (T_m) of cocrystal is often between that of the drug and the coformer, or lower than both individual T_m values. The DSC thermograms for Ibu, IsoNA, and their equimolar physical mixtures are shown in Figure 2. Ibu and IsoNA exhibited characteristic melting points, when heated using a ramp rate of 20°C/min, at approximately 80.58±0.32°C and 161.56±0.59°C, respectively. Physically mixed and ball-milled samples exhibited DSC traces devoid of an endothermic peak characteristic of IsoNA melting and importantly, a new endothermic event, considered to be the heat of fusion for a cocrystal was observed at approximately 123°C. The enthalpy associated with this peak increased in value as a result of increasing mechanical energy (physically mixed sample (50.1±0.77 J/g); 2 minutes milling (148.6±0.83 J/g); 5 minutes milling (155.6±1.02 J/g)). Moreover, ball milled samples exhibited an Ibu melting peak that was significantly depressed, decreasing from 80.58±0.32°C to 73.97±0.56°C and 72.03±0.04°C for 2 minutes and 5 minutes milling, respectively. The enthalpy of these two transitions was also significantly lowered. Moreover, there was no evidence of a melting endotherm for crystalline IsoNA in the DSC thermograms where Ibu was present. From the data, it would appear that once Ibu melted, IsoNA dissolved in the molten drug.

The addition of 10% xylitol, as shown in Figure 3, considerably decreased the

value of enthalpy associated with the cocrystal peak from 148.6±0.83 J/g to 62.46±0.64 J/g after 2 minutes milling. In this case it is important to note that the maximum enthalpy expected for the formulations incorporating 10% w/w xylitol would be approximately 133 J/g (0.9x148.6). The enthalpy observed at 2 minutes milling in the presence of 10% Xylitol was approximately 48% of what was expected. The enthalpy, nonetheless, increased significantly with increasing duration of milling, reaching 124.69±1.13 J/g (96% of value observed for neat cocrystallisation) after 45 minutes of consecutive milling. A further 15 minutes milling processing, however, decreased the measured cocrystal ΔH to 107.25±0.98 J/g. In all cases, there was a clear melting endotherm present for Xylitol suggesting that, unlike IsoNA, it remained crystalline following Ibu melting.

Hot Melt Extrusion

Hot melt extrusion is a non-ambient process that forces materials through a heated barrel. Processing parameters and formulation variables have a significant impact upon the properties of extruded product. The process parameters and associated observations made during HME are listed in Table 1. The incorporation of polymeric matrix carriers (formulations 2 and 3) significantly reduced the torque values, when compared with formulation 1 (Net cocrystal reagents). The addition of 10% w/w xylitol resulted in an increase of torque from 40-44Ncm up to 109-122Ncm and a reduction in the residence time from 233s to 90s. A further increase in the xylitol concentration to 30% w/w decreased the torque to 43-59Ncm, similar to the torque values recorded for formulation 1. A further increase in the concentration of xylitol to 50% w/w reduced the torque to 19-22Ncm. Interestingly, decreasing torque values progressing through formulations 4, 5 and 6 resulted in residence times that were increased. The addition of xylitol (30% and 50%) increased residence time to 272s and 329s, respectively.

Thermal Analysis

When using conventional DSC at a heating rate of 20°C/min during preliminary study, physically mixed Ibu and IsoNA blends showed only endothermic events

typical of the melting of Ibu and the Ibu/IsoNA cocrystal (Figure 2). By using hyper DSC (200°C/min), however, it was possible to observe an endothermic peak characteristic of the melting of the residual IsoNA content. The thermograms provided by hyper DSC measurements for pure Ibu, IsoNA, xylitol and their extruded mixtures are presented in Figure 4. Ibu and IsoNA exhibited characteristic melting points (peak) at 84.41±0.57°C and 163.26±0.99°C, respectively, when heated using a ramp rate of 200°C/min. The DSC trace obtained for the reference cocrystal, precipitated from solution, showed one single endothermic event, typical of a melting transition ranging from 120.78±0.03°C to 134.59±0.43°C, with the peak maximum at 127.29±0.55°C.

At such relatively fast heating rate, xylitol melted at 104.17±0.29°C and displayed a broad melting peak ranging from 92.98±0.13°C to 112.30±0.17°C. The similarity of melting temperatures for xylitol and the cocrystal presented difficulty in using DSC to determine presence of cocrystal. This was made more difficult by the fact that the melting transition associated with the cocrystal showed considerable depression if measured in the presence of xylitol (Figure 4). This was particularly relevant in formulations containing high concentrations of xylitol. Moreover, evidence of unreacted Ibu and IsoNA could be observed in thermograms associated with suspensions of 30% and 50% xylitol. However, T_m of the residue of both parent components were also noticeably depressed (both onset and end point).

Amorphous carriers Eudragit® E PO and Soluplus® showed a T_g at 43.94±0.13°C and 66.52±0.20°C, respectively (Table 2). All carrier excipients studied were thermally stable whereas ibuprofen and the reference cocrystal showed onset of decomposition at 197.44±3.67°C and 164.07±6.77°C, respectively.

PXRD

PXRD patterns are depicted in Figure 5. Ibu showed distinct peaks at 6.3°, 16.7°, 20.2° and 22.4° 2Θ, ISoNA at 17.9°, 21.0° and 23.4° 2Θ, and Xylitol at 20.0°, 22.5°, 22.7° and 38.4° 2Θ, respectively. For the physically mixed systems the PXRD data (iv) correlated well with DSC data in that there was little evidence of cocrystal formation. For the extruded formulations containing Xylitol, the

cocrystal product (V-X) showed distinct peaks that were distinguishable from simple overlap of cocrystal reagents and xylitol. New peaks were evident at 3.3° and 17.1° 2Θ. The intensity of the peaks attributable to cocrystal product varied as a function of excipient type and concentration. It is evident from cocrystal yield that the conversion from the parent reagents to the cocrystal was 28.06±1.65%, 33.46±0.55%, 28.60±0.61% and, 28.25±0.65% for formulations 1, 4, 5 and, 6, respectively. Those formulations extruded with polymeric excipient, on the other hand, showed no evidence of cocrystal formation. Interestingly, these diffractograms (vi and vii) showed no characteristic peaks attributable to Ibu either. This would suggest that Ibu had been rendered amorphous following extrusion.

FTIR Spectroscopic Analysis

The FTIR spectra, in the 3600-2600 cm^{-1} and 2000-1200 cm^{-1} wavenumber intervals, for Ibu, IsoNA, xylitol, the cocrystal reference, and the extruded suspensions containing 10%, 30% and, 50% xylitol, respectively, are represented in Figure 6. The assignment of IR vibrational bands in Ibu, IsoNA and the equimolar reference cocrystal obtained from solution method is listed in Table 3. The FTIR spectrum for Ibu showed a number of weak peaks in the wavenumber region [3100-2900 cm^{-1}] reflecting complex modes of vibrations associated to C-H, C-H_2 and C-H_3 groups[49]; and a very broad peak covering almost the whole wavenumber range from 3400~2800 cm^{-1} associated to O-H stretching vibrations within a carboxylic acid dimeric structure of Ibu. A sharp and intense C=O stretching band at 1721.16 cm^{-1} was also observed for Ibu due to the presence of a mono carboxylic acid group[50]. IsoNA, on the other hand, showed characteristic IR bands at: (i) 3369.03 cm^{-1} and 3185.83 cm^{-1}, representing asymmetric and symmetric ν_{N-H} stretching vibrations, respectively, for the H-bonded primary amide groups among closely packed IsoNA molecules[51,52]; (ii) 1668.12 cm^{-1}, denoting $\nu_{C=O}$ stretching of the amide carbonyl group[53]; (iii) 1622.80 cm^{-1} and 1594.84 cm^{-1} for the δ_{N-H} bending vibrations of the primary amide[54]; and (iv) 1551.45 cm^{-1} signifying $\nu_{C=N}$ ring stretching in the heterocyclic pyridine ring structure[54,55].

As shown in Figure 1, the the cocrystal structure involves a number of groups with characteristic IR vibrational bands. They are the IsoNA amide N-H (stretching and bending), the ISoNA amide C=O (stretching), and the pyridine N of isoNA, as well as the carboxylic acid group of IBU.

The amide carbonyl and the pyridine N are two competing H-bond acceptor sites in IsoNA structure. The pyridine N, however, is generally considered a better acceptor[56], and hence more prone to attract the amide H-atom, forming a N-H•••N bond in bulk IsoNA. In forming an amide homodimer synthon during cocrystallisation, the amide N-H asymmetric and symmetric stretching (3369.03 cm^{-1} and 3185.83 cm^{-1}) were shifted to 3434.60 cm^{-1} and 3173.29 cm^{-1}, respectively, whilst the amide carbonyl stretching vibration band (1668.12 cm^{-1}) was shifted to 1629.55 cm^{-1}. The N-H blue shift to 3434.60 cm^{-1} indicated dissociation of the existing N-H•••N bond, generating free amide N-H. The N-H red shift to 3173.29 cm^{-1}, together with the carbonyl red shift to 1629.55 cm^{-1}, were both attributed to the formation of N-H•••O bonds between the amide N-H and amide carbonyl groups in the IsoNA homodimer.

The lone pair of electrons on the pyridine N, after dissociation of the original N-H•••N bond in bulk IsoNA, provides a strong proton acceptor site. The absence of the associated Ibu O-H stretch (broad peak in the region 3400~2800 cm^{-1}) provides support for dimeric dissociation in bulk Ibu. The occurrence of an additional peak at 3317.93 cm^{-1} was attributed to the formation of a supramolecular heteromeric synthon through O–H•••N hydrogen bonding between the pyridine N and the Ibu O-H[38]. Moreover, in forming the carboxylic acid-pyridine H-bond, the carboxylic acid carbonyl (1721.16 cm^{-1}) was red shifted to 1702.84 cm^{-1}, while a C-H stretching (796.457 cm^{-1}) from the pyridine ring was also red shifted to 779.101cm^{-1}, indicating formation of a C–H•••O hydrogen bond within the heteromeric synthon[39,57]. It was also apparent that the addition of xylitol as a matrix carrier did not alter interactions between two parent cocrystal reagents. The IR spectra of the cocrystal/xylitol suspensions were typical of the spectrum of cocrystal with xylitol superimposed (Figure 6).

Raman Spectroscopy and Mapping

As shown in Figure 7, the unprocessed Ibu, IsoNA, and their equimolar cocrystal showed three distinctive peaks within Raman shift region 1050.0~975.0 cm^{-1}. Ibu exhibited a peak at 1006.13 cm^{-1} characteristic of aromatic ring C-C stretching. IsoNA presented a very intense and well-defined peak at 993.97 cm^{-1} attributed to the pyridine ring structure. In the equimolar cocrystal, the pyridine peak was broadened and the wavenumber was shifted to 1020.50 cm^{-1}. There were two shoulders characteristic of the vibration of the aromatic ring of Ibu, as well as the residual pyridine ring structure from the remaining free IsoNA. The matrix carrier xylitol, on the other hand, did not show any distinctive peak within this Raman shift region. It is, therefore, clear that the peak at 1020.50 cm^{-1}, characteristic of the cocrystal, is free of interference from any other component within the formulation. By plotting the intensity of this specific peak across the the sampled cross-sectional area of the extrudate we can determine the distribution of the cocrystal.

Figure 8 (a) provides a Raman map of the extrudate produced using only cocrystal reagents devoid of any excipient. The peak intensity at 1020 cm^{-1} has been used to generate the Raman map using a rainbow cubic look-up table. The lookup table was generated within an ordinate range of [1000-7500 INT]. It is apparent that there is a difference in the intensity of the cocrystal peak across the cross-sectional area with a highly intense region focused to the outer edges of the extrudate. The spectra of a number of labelled points, representing a range of intensities across the map are provided for comparative purposes.

The mapping results shown in Figure 9 depict the intensity values of the 1020.50 cm^{-1} peak in extrudates containing different concentrations of xylitol and following storage. Interestingly, the intensity of the cocrystal peak varied considerably as a function of xylitol concentration and storage. When extruded with 10% xylitol (Figure 9(1)), there was an obvious and significant increase in the intensity of cocrystal (relative to neat extrusion) across the cross-sectional area of the extrudate. This result correlated well with results obtained from XRD where the formulations containing 10% xylitol had intense diffraction bands at 3.3° and 17.1°. With increasing xylitol concentration in the formulation (30% and 50%, respectively), the overall intensity for the characteristic cocrystal peak

at 1020.50 cm^{-1} decreased throughout the entire cross-section (Figure 9, (2) and (3)). This result was again mirrored in the XRD where the cocrystal yield decreased from 33.46±0.55% to 28.25±0.65%, as the concentration of xylitol increased from 10% to 50%. Importantly, after 12-month storage under controlled conditions (20°C with 70% RH), an extensive increase in the intensity values for the distinctive cocrystal peak at 1020 cm^{-1} was observed for all three formulations containing xylitol (Figure 9, (4), (5) & (6)), suggesting significant growth of the cocrystal content upon aging .

Cocrystal Morphology Study

The crystal habit of a drug is extremely important consideration in pharmaceutical manufacturing. Typically a number of basic physicochemical properties such as solubility, dissolution rate, powder flow, compressibility, and mechanical strength depend on the crystal habit. Figure 10 cshows polarised light micrographs of Ibu, as received, cocrystal formed using traditional solvent methods and melt extruded cocrytal particles. The PLM images clearly depict the needle-like shape of both Ibu and the reference cocrystal standard. Such anisotropic shape could be problematic during pharmaceutical manufacturing [58,59]. Conversely, the melt-extruded cocrystal particles (Figure 10c), were uniformally shape and much smaller in size.

In-vitro Drug Dissolution

Drug release profiles (Figure 11) and associated data confirmed that all extruded formulations exhibited improved solubility and increased dissolution rate of Ibu with the exception of the formulation containing Eudragit® E PO. The amorphous dispersion with Soluplus® (formulation 2) had a similar relative dissolution rate at 5 min (0.95±0.06) and 45 min (0.44±0.04) to the neat-extruded formulation 1 (0.94±0.04 and 0.44±0.00, respectively). Formulation 1, however, had a significantly higher dissolution rate (0.20±0.01) and increased solubility (DP_{180min} of 36.30±1.33%) at 180 min than formulation 2 (0.16±0.02, and 29.08±3.13%, respectively). The inclusion of xylitol significantly increased the dissolution rate at drug percent released. In particular, the extruded suspension containing 50% w/w xylitol (formulation 6) exhibited the highest DP and RDr

values of all formulations (DP_{5min} at 6.41±0.07%, DP_{45min} at 37.41±0.81%, DP_{180min} at 43.53±0.34%, RDr_{5min} of 1.28±0.01, RDr_{45min} of 0.83±0.02 and, RDr_{180min} of 0.24±0.00, respectively.

Cocrystal Content Evaluation After Aging

The stability of pharmaceutical materials that may undergo physical form change during storage is fundamentally important. Stability must be examined in detail in order to develop successful pharmaceutical products. The physical stability relating to the relative quantity of cocrytal is shown in Figure 12. Samples were stored at room temperature under both desiccated and humid conditions (20°C over silica gel, and 20°C with 70%RH, respectively) to evaluate changes in the cocrystal content. As previously presented, formulation 4 that contained 10% w/w xylitol showed a significantly higher cocrystal yield (33.46±0.55%) than the neat-extruded formulation 1 (28.06±1.65%) immediately after HME processing. Increasing the concentration of xylitol considerably decreased the yield for formulations 5 (28.60±0.61%) and 6 (28.25±0.65%), respectively. A similar but qualitative indication was also evident in the Raman maps. Interestingly, the neat extruded formulation 1 showed an increase in cocrystal yield increase following 12-month storage under dry (33.85±2.69%) and humid (43.31±1.25%) conditions, respectively. Formulations containing xylitol, retained the same quantity of cocrystal yield following storage under dry conditions, while showing increase to various extents, 34.86±0.85%, 35.66±1.88% and 34.49±2.40 for formulations 4, 5 and 6, respectively, following storage under humid conditions.

Discussion

Pharmaceutical cocrystals offer a way to overcome the solubility issues associated with BCS class II compounds while also retaining the thermodynamic stability of the crystalline form of a drug[60,61]. Conventionally, the manufacture of a pharmaceutical cocrystal product is divided into two major aspects: the production/synthesis of the cocrystal itself and the subsequent formulation of cocrystal into a pharmaceutical dosage form. Pharmaceutical cocrystals have developed significantly in the past decade with increasing number of patents issued worldwide. However, at present there is still limited marketed examples

of pharmaceutical products involving cocrystals[62,63]. With the recent implementation of techniques such as hot-melt extrusion[28] and spray drying[64,65], as methods of manufacturing pharmaceutical cocrystals, it has become possible to combine cocrystallisation and formulation to reduce the number of manufacturing steps involved in drug product manufacture. Hot-melt extrusion is particularly advantageous owing to its continuous processing capability; ease of scaling and it may be used to manufacture cocrystals without the need for organic solvents.

To achieve mechanochemical synthesis of cocrystals via HME comprehensive investigations must be conducted in order to develop a thorough understanding of the reaction selectivity between ingredients; the most appropriate reaction conditions/parameter settings for a specific system; and most importantly, the selection of a suitable matrix for the cocrystal reagents. To probe this further, we have processed mixtures consisting of chosen cocrystal reagents and an 'inert' carrier excipient via hot melt extrusion. The principal hypothesis being that Ibu/IsoNA cocrystals should be suspend in the final matrix. Consequently, the HME processing temperature was set significantly lower than the T_m onset of the cocrystals (approximately 120°C). The chosen carrier excipient was either a pharmaceutical grade polymer (Eudragit® EPO and Soluplus®) with relatively low values of Tg hence lower processing temperature, or a commonly used food and pharmaceutical additive, namely Xylitol, that was molten at the chosen extrusion temperature.

For Soluplus® and EPO there was evidence of crystalline IsoNA within the matrices and negligible Ibu/IsoNA cocrystal product. Moreover, for both polymeric systems, there was no evidence within XRD patterns of crystalline Ibu, after extrusion. In the case of Soluplus®, the lack of crystalline Ibu may be attributed to heating the drug beyond its melting point during extrusion (92°C) and entrapping the drug in a highly viscous polymer network. The entrapment of Ibu molecules within rubbery and highly viscous Soluplus® would lead to reduced mobility of Ibu and consequently reduce the interaction with IsoNA, limiting cocrystal yield. Conversely, when utilising EPO as a matrix carrier, competition between EPO and the coformer isonicotinamide to form hydrogen bonds with ibuprofen would further impact upon cocrystal yield. There have

been many reports of interactions between carboxylic acids and EPO[66–68]. Additionally, we would expect, as with Soluplus®, that the mixing of Ibu with highly viscous rubbery EPO would physically hinder molecular interaction between the cocrystal reagents limiting cocrystal yield.

Conversely, the small molecular weight sugar alcohol used in this study (xylitol), was found to assist cocrystallization. In part, this may be attributed to limited miscibility between cocrystal product and Xylitol. Indeed, polyols have been shown previously to be relatively inert during extrusion[69]. Furthermore, it is well accepted that low molecular weight solvents (typically volatile organic solvents) can significantly improve cocrystal yield. There are many reported articles describing the significant increase in yield associated with solvent-assisted-methods relative to neat preparation[17,70,71]. In comparison to Soluplus® and EPO, Xylitol is a low molecular weight (152 g/mol) carrier, with a melt viscosity typically 3~4 orders of magnitude lower than the two polymeric excipients. The lack of miscibility between the cocrystal and xylitol and the low viscosity and hence, increased molecular mobility of cocrysal reagents appear to have been key drivers in the successful production of cocrystal. Moreover, the low viscosity, ease by which cocrystal may disperse throughout the melt[58] and the rapid solidification of xylitol post-extrusion, led to a solid extrudate with cocrystal well dispersed throughout the xylitol matrix.

Cocrystals formed using xylitol as a matrix carrier possessed the same hydrogen-bonding pattern (FTIR) and crystal structure (XRD) as the reference cocrystal manufactured via solvent evaporation and the neat-extruded cocrystal . The inert nature of xylitol and the limited miscibility with the cocrytal is fundamental to successful cocrystal formation during extrusion. Strong non-covalent interactions between any ingredients, other than a coformer pair, may be detrimental to product formation and yield. Therefore, it becomes very important to understand and if necessary quantify the strength of interaction between all components to ensure successful cocrystal formation during extrusion.

From this work, it is evident that cocrystal suspensions may be successfully manufactured in a single step using extrusion provided a matrix carrier has specific qualities. Potential matrix carriers should have limited ability to form

660 non-covalent interactions with all cocrystal components, a sufficiently low
661 processing temperature such that it is lower than cocrystal melting temperature
662 and rapid solidification upon cooling.
663 The improvement in the dissolution of drug compounds, when manufactured
664 as cocrystals, can be used to enhance the solubility of BCS class II drugs. It was
665 evident that the addition of small quantities of xylitol (10%) increased cocryatl
666 yield however at higher xylitol concentrations (30% and 50%), the cocrystal
667 yield was equivalent to the formulation devoid of xylitol (Formulation 1). There
668 was no evidence of crystalline ibuprofen immediately after processing, indicating
669 that residual ibuprofen was rendered amorphous. Therefore, the amorphous
670 content (as percentage of the total Ibu content) in the 30% and 50% xylitol
671 formulations were equivalent to that in the neat-extruded formulation. And the
672 amorphous Ibu content in the 10% xylitol formulation was less than that in the
673 system devoid of xylitol.
674 In drug dissolution studies, formulation 1 (devoid of xylitol) exhibited
675 significantly increased rate and extent of drug release relative to the crystalline
676 ibuprofen powder. This could be the result of a combined effect of the formation
677 of both the cocrystal and amorphous forms of ibuprofen. Although it is difficult
678 to quantify the impact of each individual form to the dissolution improvement,
679 the fact that formulations 1, 5 and 6 all had equivalent amounts of cocrystal yield
680 is suggesting that the further increased dissolution rates of formulations 5 and 6,
681 relative to formulation 1, are attributed to the presence of xylitol.
682 The enhanced dissolution rate observed for a cocrystal suspension embedded
683 in a hydrophilic matrix relative to neat cocrystal powders may be attributed to
684 (1) the cocrystal particles present in the suspension are less aggregated due to
685 the distribution within the matrix carrier, facilitated by agitation caused by
686 extrusion screw rotation and (2) improved wettability owing to the
687 hydrophilicity of the carrier[42,72–75]. For the matrix containing Soluplus®, the
688 release of Ibu initiated rapidly due to the presence of amorphous Ibu at the
689 surface of the Soluplus® matrix. However, the erosion of the Soluplus® matrix
690 was significantly slower than that of formulations containing xylitol or those
691 devoid of excipient. With IsoNA rapidly dissolving into the dissolution medium
692 due to its high aqueous solubility, the rapid ingress of water into the Soluplus®

matrix may have increased Ibu mobility causing clustering of the dispersed Ibu molecules and their subsequent recrystallization within the matrix. Conversely, the formulation containing EPO, exhibited a reduced dissolution rate. This retardation of drug release may be due to the cationic nature of the polymer, the interaction with the acidic drug and the inherent slow dissolution of the polymeric carrier in the chosen dissolution media.

Many approaches have been used to enhance the dissolution performance of BCS class II drugs. Cocrystals have not only been shown to improve drug release properties but are also more physically stable than amorphous drug forms during storage. To understand the storage stability of the extrudates cocrystal suspensions were desiccated under two different conditions, namely, a dry environment over silica gel, and humid condition maintained at 70%RH, both at 20°C for 12 months. As previously discussed, hydrogen bonds between the two cocrystal reagents are stronger than that between the homo-molecules[6,41], it is therefore of relevance to confirm if the formed cocrystal could stay unchanged under pharmaceutically relevant storage conditions. Indeed, both Raman mapping and PXRD patterns showed that the stored samples had varying degrees of cocrystal growth as a result of aging. This is quantitatively indicative of incomplete cocrystallisation during extrusion. However, both DSC and PXRD analyses on extrudates immediately following manufacture showed little evidence of the presence of crystalline Ibu or IsoNA. The growth of cocrystal during storage may be attributed to interaction between amorphous Ibu and IsoNA molecules, that subsequently form cocrystals[76]. The samples stored under high humidity, in particular, showed significant cocrystal growth during storage most probably due to increased global molecular mobility following ingress of moisture into the xylitol matrix. Consequently, it may be concluded that even if reagents are partially amorphous following extrusion and are physically stabilised by the presence of a matrix carrier they may still recrystallize. This is driven by the ingress of moisture, the drop in Tg, associated increase in molecular mobility of the amorphous components[77] and the subsequent formation of a thermodynamically favourable cocrystal product.

Furthermore, the incomplete cocrystal conversion may be attributed to the rapid transport of material through the extrusion barrel, limiting reaction time.

The residence time of a typical HME process is a multifactorial-controlled variable that is dependent upon factors such as the properties of the extruded materials, the processing parameter settings and, the machine geometry[78–82]. For larger scale extruders, residence time may be prolonged due to physically extended barrel length. Limitation with respect to limited reaction time may be overcome using increased mixing intensity. An incorrect choice of screw geometry may lead to inadequate mixing in the barrel and reduce cocrystal yield[27,28]. The extruder utilized in this work consisted of a 10cm long conical barrel coupled with non-intermeshing conical co-rotating screws. A full conveying screw design was employed throughout the entire length of the barrel. With this set-up, the compression of materials occurs by decreasing the barrel volume in the direction of melt flow. When extruding a cocrystal suspension from a mixture of the reagent pair and a chosen carrier, however, such an extruder design (limited mixing intensity) may not be aggressive enough to compensate for the limited residence time In addition, it may also be important to consider the solubility of cocrystal parent reagents in the carrier. A liquefied carrier that cannot solubilize the parent reagents may reduce interspecies collision. Conversely, carrier-reagent reactivity should be less than reagent-reagent reactivity in order to encourage increased cocrystal yield. Theoretically, the solubility of the components within this process would be expected to be temperature dependent. Thus a detailed investigation into the influence of processing temperature on the solubility between components and hence the cocrystal conversion is necessary.

Conclusion

This work demonstrated the viability of concurrent cocrystallisation and drug product formulation in a miniature scale (10g) co-rotating twin-screw extruder. The final extrudates were examined to be intimate mixtures wherein the newly formed cocrystal particulates were physically suspended in a matrix formed by a 'inert' carrier excipient. Importantly, it was established in this study that an appropriate carrier for a cocrystal reagent pair during HME processing should satisfy certain criteria including: (1) limited interaction with parent reagents and cocrystal product; (2) processing temperature sufficiently lower than the onset

of cocrystal T_m; (3) low melting viscosity; and (4) fast solidification upon cooling. In conclusion, the use of low viscosity, chemically 'inert' matrix carriers may be successfully employed in the mechanochemical synthesis of pharmaceutical cocrystal suspensions via HME.

Figures

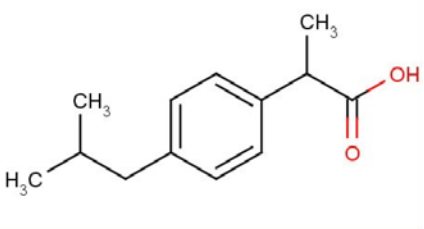

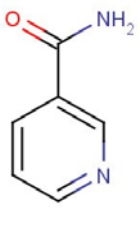

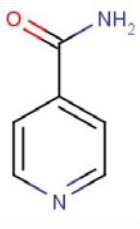

Ibuprofen Nicotinamide Isonicotinamide

(a)

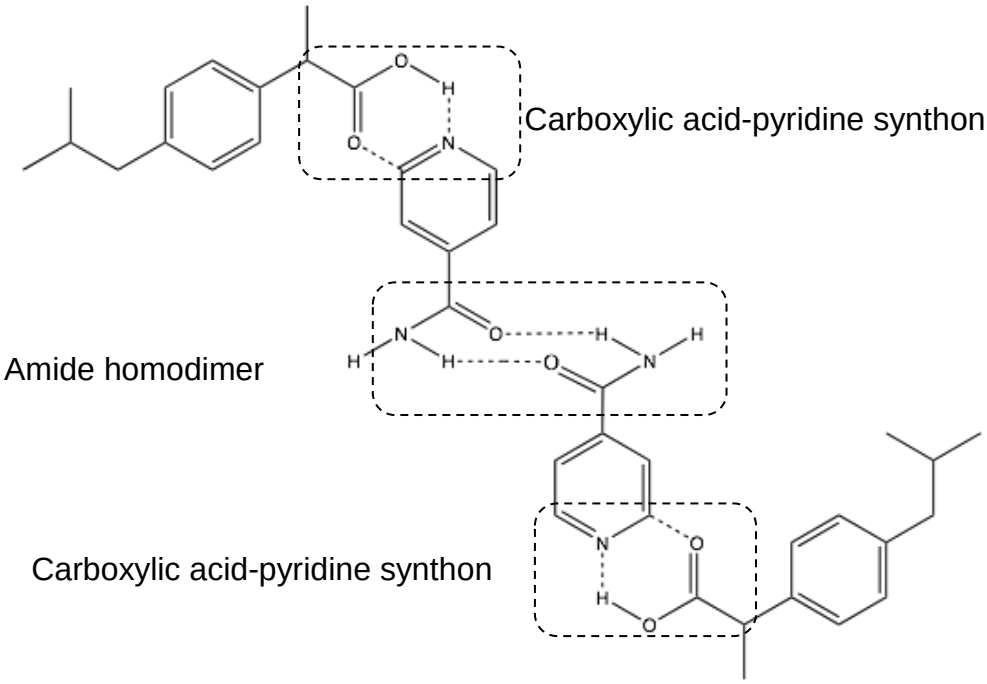

(b)

Figure 1(a). Molecular structure of Ibuprofen, nicotinamide, isonicotinamide and **(b)** proposed theoretical architecture of an ibuprofen/IsoNA cocrystal (FriŠčić & Jones 2007, Karki et al; 2007). Hydrogen bonds are shown as dotted lines.

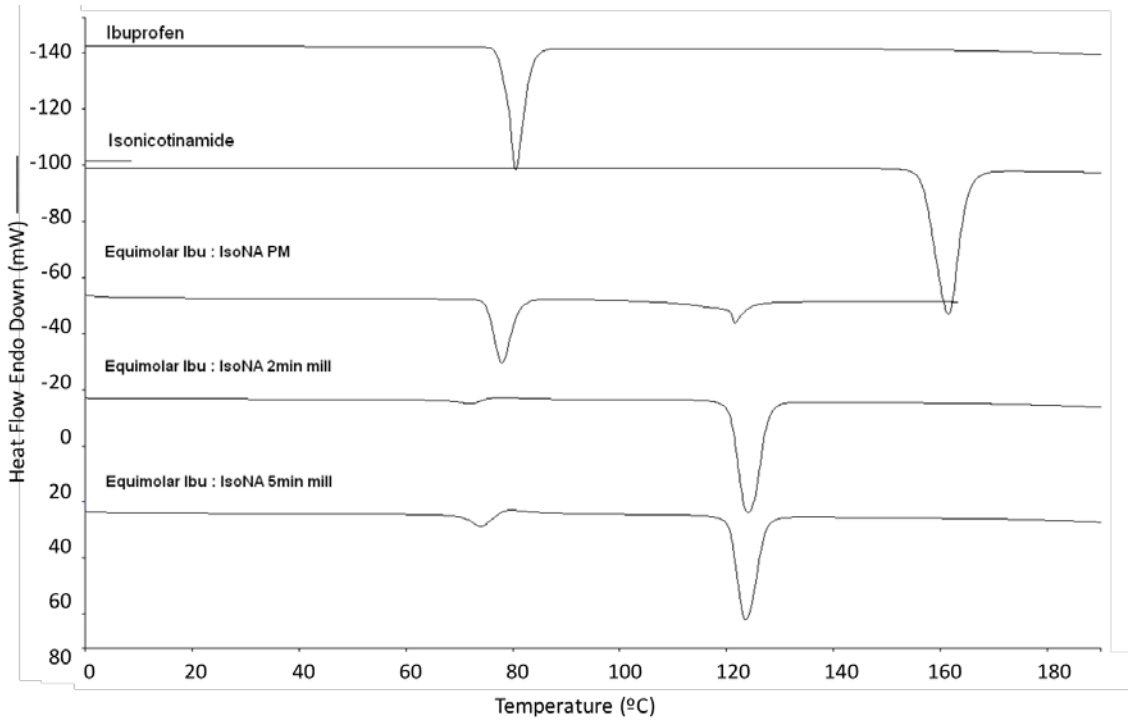

Figure 2 Representative DSC thermogram from top to bottom: crystalline ibuprofen; crystalline isonicotinamide (as is); physical mixture (PM) of ibuprofen & isonicotinamide at 1:1 molar ratio; equimolar Ibu/IsoNA ball milled for 2 minutes; and equimolar Ibu/IsoNA ball milled for 5 minutes.

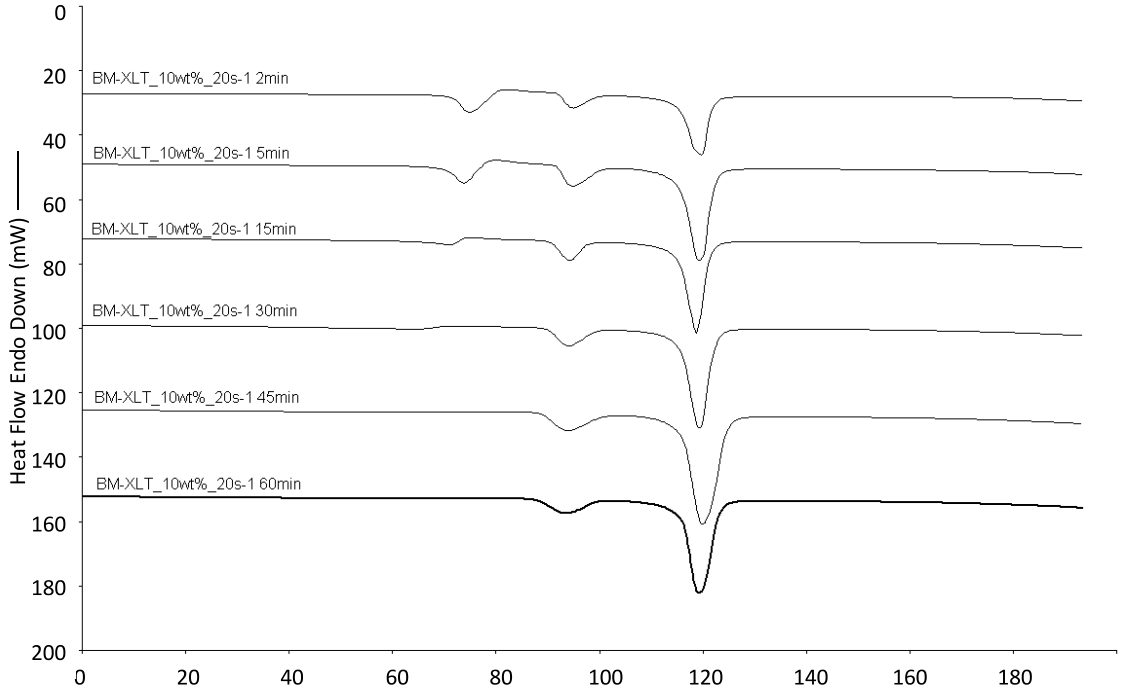

Figure 3 Overlaid DSC thermograms showing the formation and increase of Ibu/IsoNA cocrystal in the presence of 10wt% xylitol after (from top to bottom): 2, 5, 15, 30, 45 and, 60 minutes ball milling.

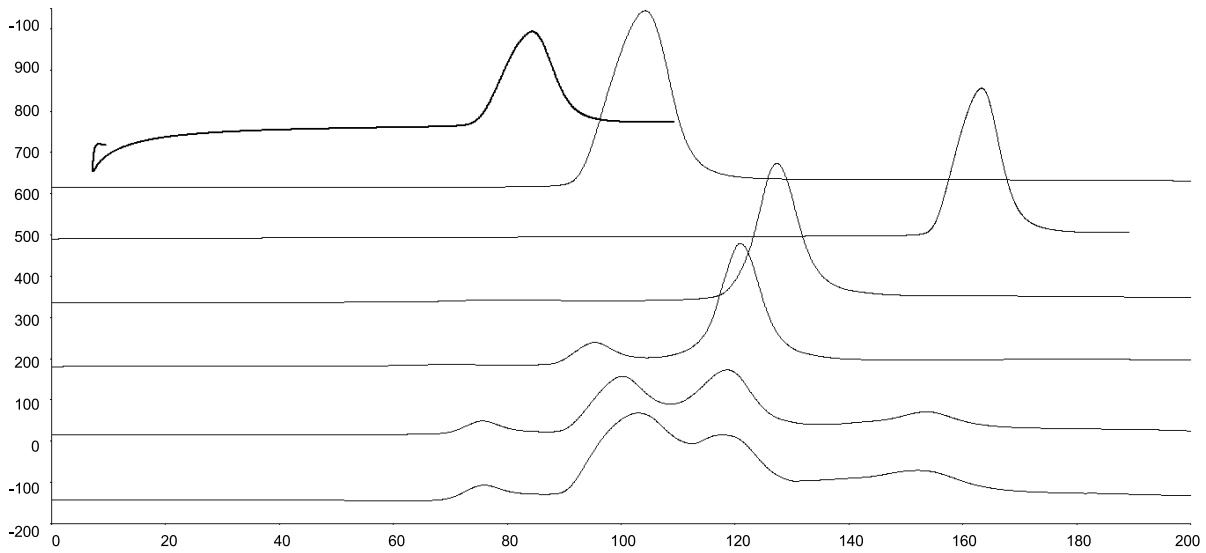

Figure 4 Representative DSC thermograms of materials used in cocrystal formulation development. From top to bottom: ibuprofen, xylitol, isonicotinamide, reference cocrystal standard prepared using solution method, extruded Ibu/IsoNA cocrystal suspension in 10wt% xylitol; extruded Ibu/IsoNA cocrystal suspension in 30wt% xylitol and, extruded Ibu/IsoNA cocrystal suspension in 50wt% xylitol.

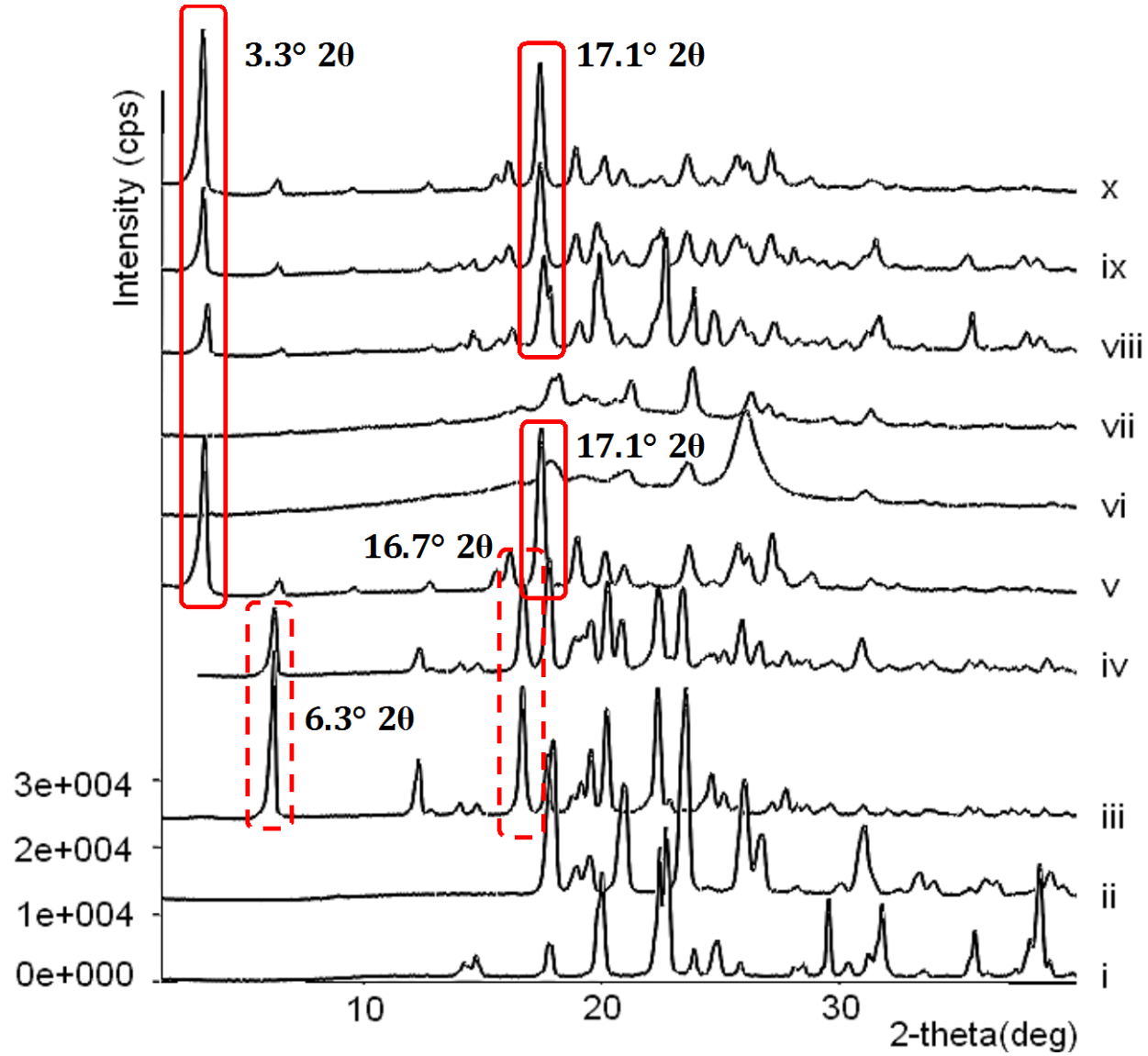

Figure 5 Overlaid PXRD patterns of: (i) xylitol; (ii) IsoNA; (iii) Ibu; (iv) equimolar Ibu/IsoNA physical mitxture; (v) 1:1 neat extruded at 92°C; (vi) 10wt% Soluplus® HME; (vii) 10wt% EPO HME; (viii) 50wt% xylitol HME; (ix) 30wt% xylitol HME; and (x) 10wt% xylitol HME. Please note: all extrudates contained ibuprofen and isonicotinamide at a 1:1 molar ratio.

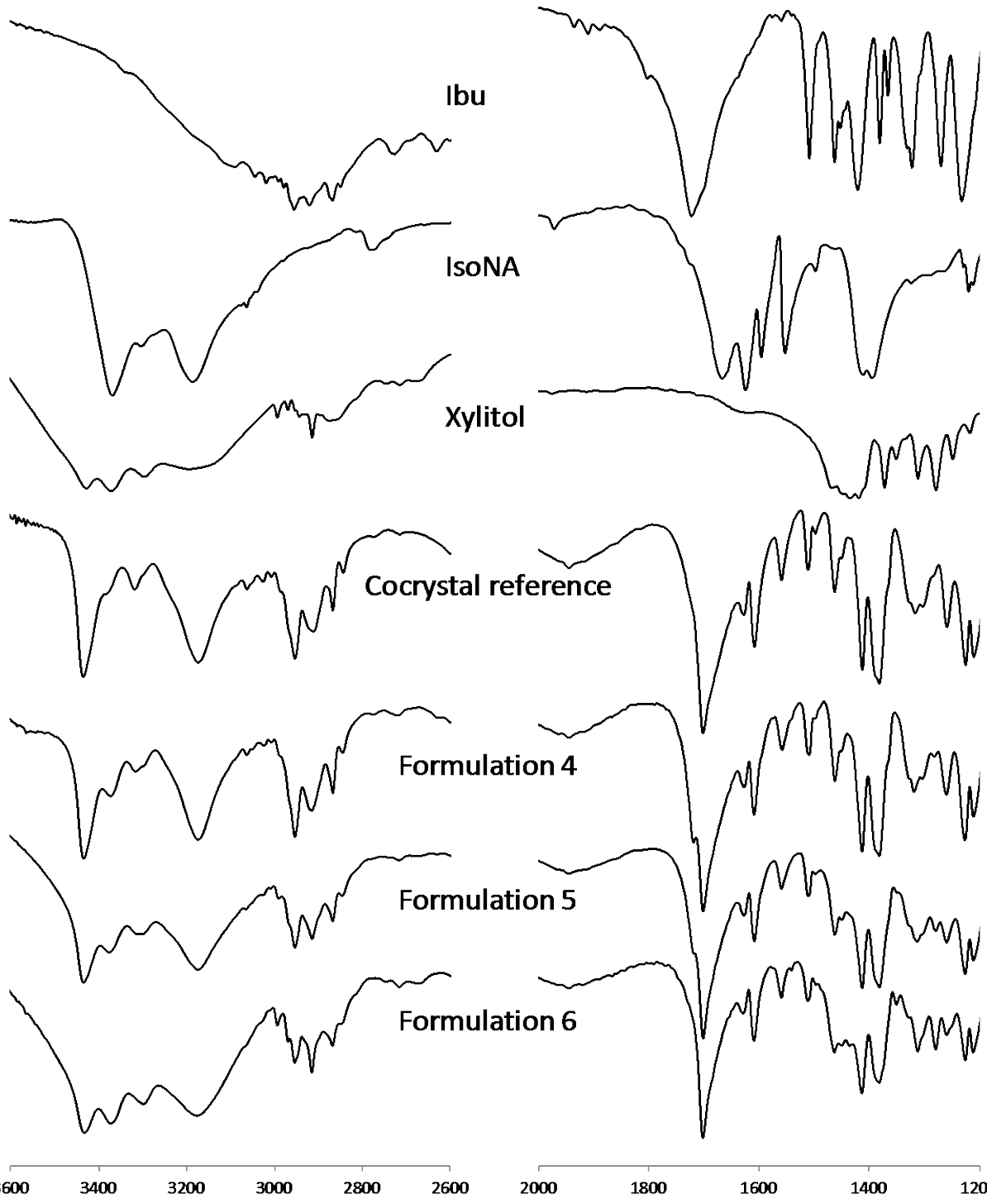

Figure 6 Overlaid FTIR spectra within wavenumber ranges of [2600-3600 cm^{-1}] and [1200-2000 cm^{-1}], respectively for, from top to bottom: Ibu, IsoNA, xylitol, the cocrystal reference, extruded suspensions containing 10%, 30% and, 50% xylitol, respectively.

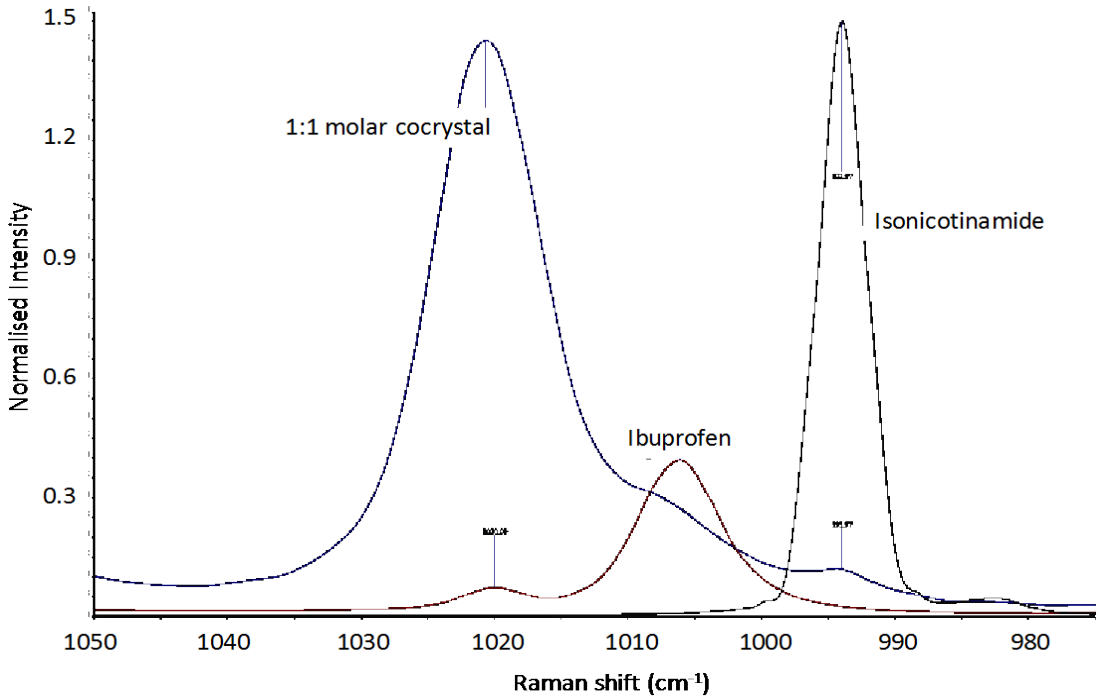

Figure 7 Raman shift region [1050.0~975.0 cm-1] showing non-interfering, characteristic peaks for: (Red) unprocessed Ibuprofen; (green) unprocessed IsoNA; and (blue) the equimolar cocrystal prepared using slow evaporation.

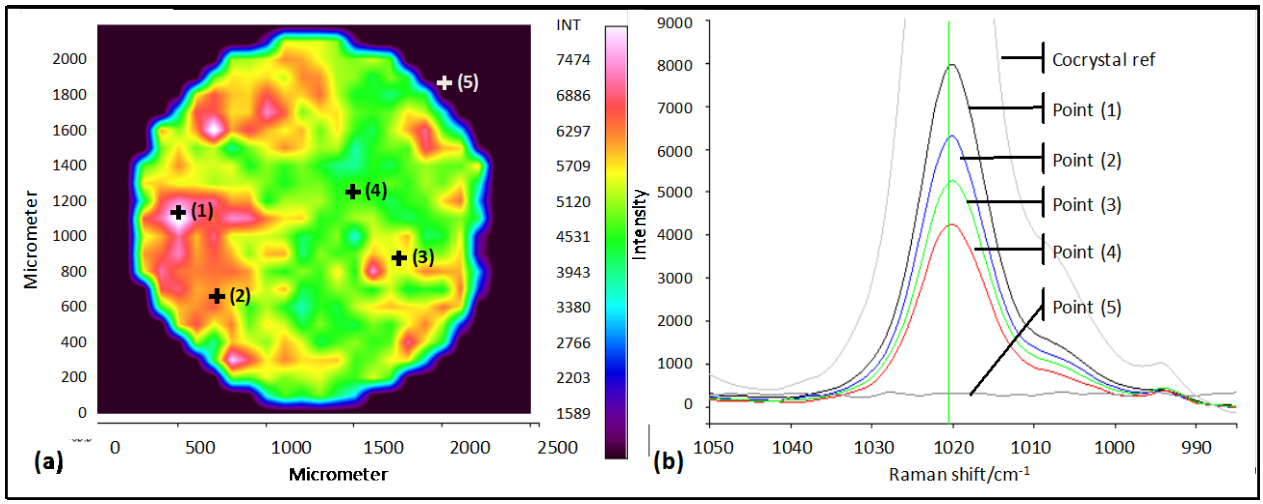

Figure 8 (a) Schematic demonstration of the occurrence and concentration of the cocrystal across the cross section of a formulation 1 extrudate. **(b)** The spectra showing the intensity of the cocrystal peak at 1020 cm^{-1} at the labelled points and that of the cocrystal reference are shown in the right figure in an overlaid format.

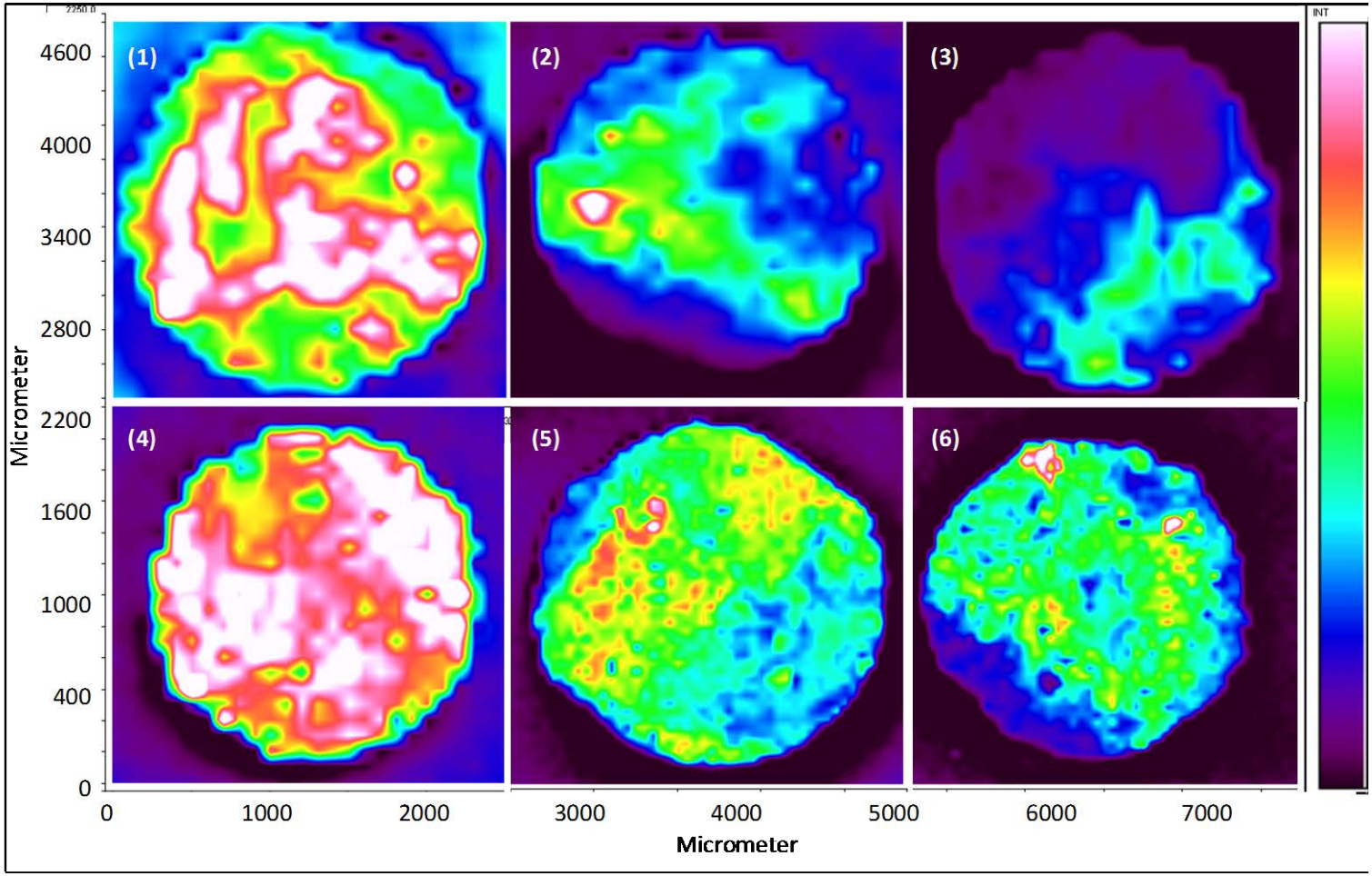

Figure 9 Raman map/image showing the intensity of the peak at 1020 cm^{-1}, characteristic of the cocrystal, throughout the cross section of: (1) fresh extrudates of formulation 4, containing 10% xylitol; (2) fresh extrudates of formulation 5, containing 30% xylitol; (3) fresh extrudates of formulation 6, containing 50% xylitol; (4) aged formulation 4; (5) aged formulation 5; and (6) aged formulation 6.

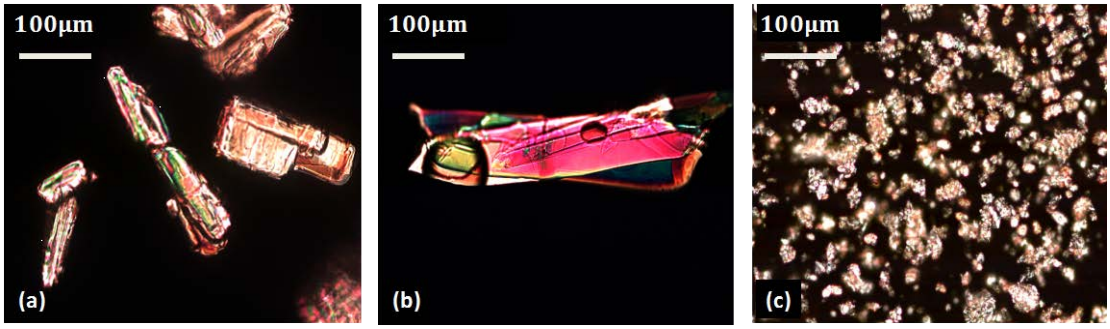

Figure 10 Polarized light micrographs showing crystal habit and size of: **(a)** unprocessed Ibu; **(b)** reference 1:1 Ibu/IsoNA cocrystal prepared using solvent evaporation; and **(c)** melt-extruded cocrystal particles. Particulates chosen all passed through 212µm sieve and were dispersed in mineral oil (200x, the entire width of each picture represents 0.5mm on a magnified scale bar).

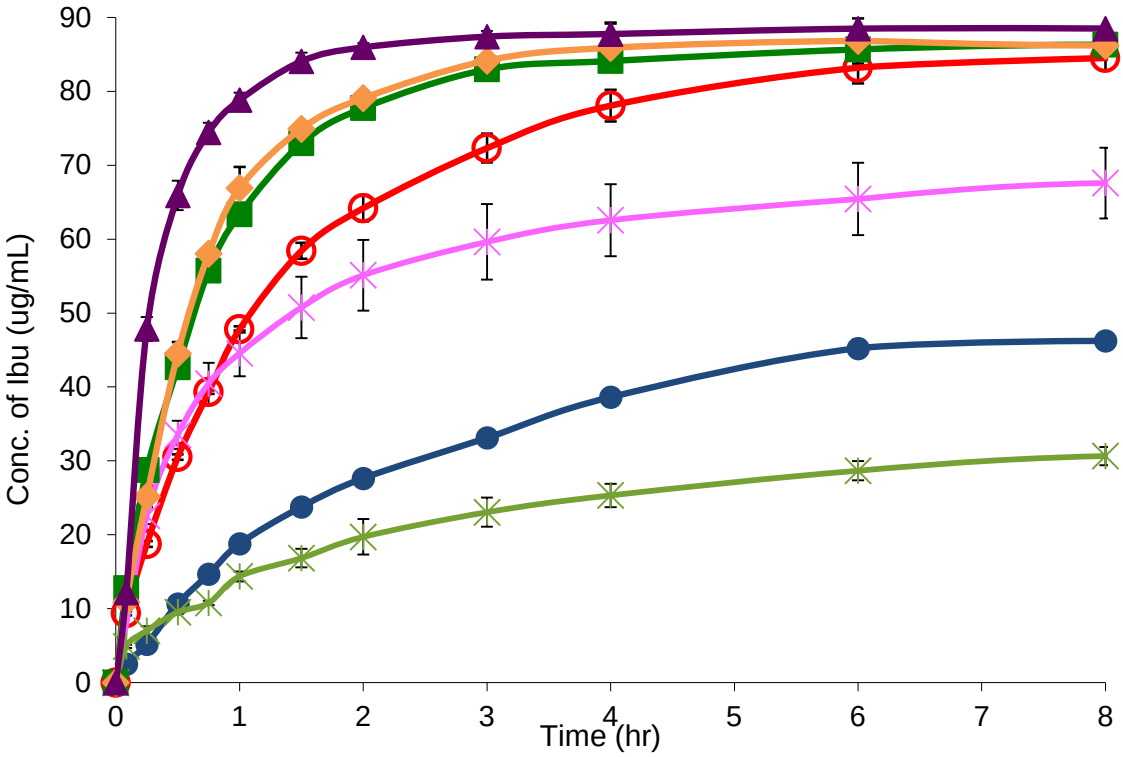

Figure 11 Drug dissolution profiles of melt extruded equimolar Ibu/IsoNA formulations in deionized water. Profiles from bottom to top: (✳) extrudates containing Eudragit® EPO; (●) Pure ibuprofen powders; (✳) extrudates containing Soluplus®; (○) 1:1 melt-extruded cocrystal (formulation 1); (■) 1:1 extruded cocrystal suspension in 10% xylitol (formulation 4); (◆) 1:1 extruded cocrystal suspension in 30% xylitol (formulation 5); and (▲) 1:1 extruded cocrystal suspension in 50% xylitol (formulation 6). Each point represents the mean ± S.D. of 3 replicates.

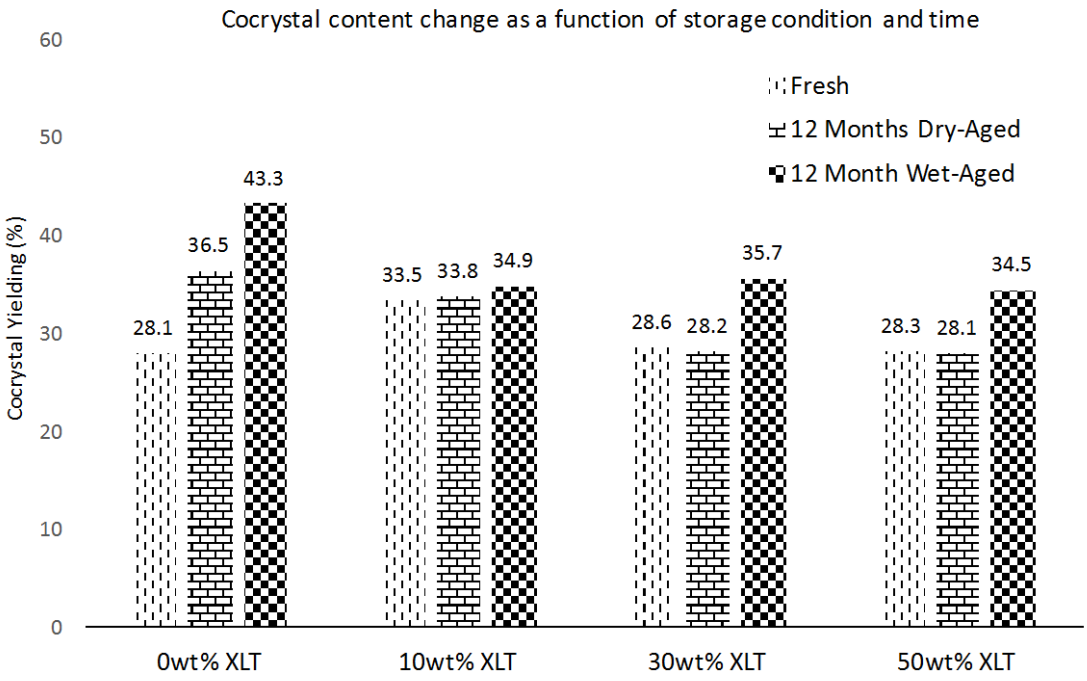

Figure 12 Yielded cocrystal content determination for freshly extruded and stored cocrystal suspension formulations containing (from left to right): 0%, 10%, 30% and, 50%, w/w xylitol.

Tables

Table 1 Nomenclature and the Parameter Settings for the Hot-Melt Extruded Formulations Composed of Equimolar Ibu and IsoNA, as well as a Third Matrix Carrier. [a]

Formula	Ibu	IsoNA	Soluplus®	Eudragit® EPO	Xylitol	Feed & Mix Temp/speed	Flushing Temp/speed	Residence time	Flush Torque	Outcome
	wt%	wt%	wt%	wt%	wt%	°C /rpm	°C /rpm	s	Ncm	
1	62.82	37.18	–	–	–	92/10	92/10	233	40~44	Fragile rods
2	56.54	33.46	10	–	–	92/10	92/10	241	4~6	Sticky strand
3	56.54	33.46	–	10	–	92/10	92/10	220	4~6	Sticky strand
4	56.54	33.46	–	–	10	92/10	85/50	90	109~122	Brittle strand
5	43.98	26.02	–	–	30	92/10	85/50	272	43~59	Brittle strand
6	31.41	18.59	–	–	50	92/10	85/50	329	19~22	Brittle strand

[a] Note that the weight ratios tabulated here provide 1:1 molar ratio for Ibu and IsoNA in the blends. The batch size was maintained at approximately 10g for each formulation and the extrudates were collected after equilibration for 5 minutes.

Table 2. The Molecular Weights, Melting/Glass Transition Temperatures and Decomposition Temperatures of Each Individual Compound used in This Study. [a]

Compound	**Mw** g/mol	**Tm or Tg** °C	**$T_{5wt\%\ loss}$** °C
Ibu	206.30	84.41 ± 0.57	197.44 ± 3.67
IsoNA	122.12	163.26 ± 0.99	188.10 ± 2.14
Ibu/IsoNA cocrystal	656.48	127.29 ± 0.55	164.07 ± 6.77
Xylitol	152.15	104.17±0.29	270.03 ± 0.43
Eudragit® E PO	47,000	43.94 ± 0.13	279.70 ± 1.00
Soluplus®	90,000~140,000	66.52 ± 0.20	308.57 ± 0.91

[a] The temperatures shown here represent the mean ± SD of three replicates. Note that the values of T_m listed the peak maximums measured at 200°C/min.

Table 3 Assignment for the Most Characteristic Vibrational Bands of Ibu and IsoNA in the Raw Materials and the 1:1 Melt-Extruded Ibu/IsoNA Cocrystal.

	IR Frequency (cm^{-1})	**Raman Shift (cm^{-1})**	**Band assignment** [a]
Ibuprofen	3400~2800	-	ν_{O-H} (Associated)
	1721.16 (vs)	1605.95	$\nu_{C=O}$ (Carboxylic acid)
	1007.62 (m)	1006.13	ν_{C-C} (Aromatic ring chain vib)
	796.457 (m)	-	$\gamma_{=C-H}$ (Aromatic ring)
Isonicotinamide	3369.03 (vs)	3070.09	ν_{N-H} (Asymmetric stretching)
	3185.83 (vs)	3063.81	ν_{N-H} (Symmetric stretching)
	1668.12 (vs)	1601.58	$\nu_{C=O}$ (Stretching)
	1622.80 (s)	-	δ_{N-H} (H-bonded amide bending)
	1594.84 (m)	-	δ_{N-H} (Free amide bending)
	1551.45 (m)	993.94	ν_{Ring} (Pyridine ring stretching)
Equimolar Ibu/IsoNA reference cocrystal	3434.60 (vs)	-	ν_{N-H} (Free amide)
	3317.93 (w)	-	ν_{N-H} (H-bonded pyridine N)
	3174.26 (vs)	-	ν_{N-H} (H-bonded amide)
	1702.84 (vs)	1612.66	$\nu_{C=O}$ (Carboxylic acid)
	1629.55 (m)	-	$\nu_{C=O}$ (H-bonded amide C=O)
	1609.31 (s)	-	δ_{N-H} (Free amide)
	1560.13 (m)	1020.70	ν_{Ring} (Pyridine)
	779.101 (m)	-	$\gamma_{=C-H}$ (H-bonded pyridine =C-H)

[a] ν = stretching vibration; δ = in-plane bending; γ = out-plane bending.

Table 4 Dissolution Parameters Calculated for Fig 11.

Formulation	Dissolution Parameters					
	DP_{5min}[a]	DP_{45min}[a]	DP_{180min}[a]	RDr_{5min}[b]	RDr_{45min}[b]	RDr_{180min}[b]
● Pure Ibu	1.26±0.17%	7.35±0.12%	16.65±0.03%	0.25±0.03	0.16±0.00	0.09±0.00
○ 1	4.69±0.19%	19.71±0.06%	36.30±1.33%	0.94±0.04	0.44±0.00	0.20±0.01
✳ 2	4.73±0.32%	19.83±1.71%	29.08±3.13%	0.95±0.06	0.44±0.04	0.16±0.02
✳ 3	2.45±0.10%	5.47±0.08%	11.64±1.36%	0.49±0.02	0.12±0.00	0.06±0.01
■ 4	5.09±0.70%	27.88±0.06%	41.90±0.04%	1.02±0.14	0.62±0.00	0.23±0.00
◆ 5	5.40±0.08%	28.74±0.18%	41.55±0.03%	1.08±0.02	0.64±0.00	0.23±0.00
▲ 6	6.41±0.07%	37.41±0.81%	43.53±0.34%	1.28±0.01	0.83±0.02	0.24±0.00

[a] DP: Drug percent (%) released at a particular time point;

[b] RDr: Relative dissolution rate (%/ minutes) at a particular time point. (RDr=DP/dissolution time).

References

(1) McNamara, D.; Childs, S.; Giordano, J.; Iarriccio, A.; Cassidy, J.; Shet, M.; Mannion, R.; O'Donnell, E.; Park, A. Use of a Glutaric Acid Cocrystal to Improve Oral Bioavailability of a Low Solubility API. *Pharm. Res.* **2006**, *23* (8), 1888–1897.

(2) Blagden, N.; de Matas, M.; Gavan, P. T.; York, P. Crystal Engineering of Active Pharmaceutical Ingredients to Improve Solubility and Dissolution Rates. *Drug Solubility How to Meas. it, How to Improv. it* **2007**, *59* (7), 617–630.

(3) Jung, M.-S.; Kim, J.-S.; Kim, M.-S.; Alhalaweh, A.; Cho, W.; Hwang, S.-J.; Velaga, S. P. Bioavailability of Indomethacin-Saccharin Cocrystals. *J. Pharm. Pharmacol.* **2010**, *62* (11), 1560–1568.

(4) Mohammad, M. A.; Alhalaweh, A.; Velaga, S. P. Hansen Solubility Parameters as a Tool to Predict Cocrystal Formation. *Int. J. Pharm.* **2011**, *407*, 63–71.

(5) Qiao, N.; Li, M.; Schlindwein, W.; Malek, N.; Davies, A.; Trappitt, G. Pharmaceutical Cocrystals: An Overview. *Int. J. Pharm.* **2011**, *419*, 1–11.

(6) Vishweshwar, P.; McMahon, J. A.; Bis, J. A.; Zaworotko, M. J. Pharmaceutical Co-Crystals. *J. Pharm. Sci.* **2006**, *95* (3), 499–516.

(7) Thakuria, R.; Delori, A.; Jones, W.; Lipert, M. P.; Roy, L.; Rodríguez-Hornedo, N. Pharmaceutical Cocrystals and Poorly Soluble Drugs. *Int. J. Pharm.* **2013**, *453* (1), 101–125.

(8) Basavoju, S.; Boström, D.; Velaga, S. Indomethacin–Saccharin Cocrystal: Design, Synthesis and Preliminary Pharmaceutical Characterization. *Pharmaceutical Research*. Springer Netherlands 2008, pp 530–541.

(9) Leyssens, T.; Tumanova, N.; Robeyns, K.; Candoni, N.; Veesler, S. Solution Cocrystallization, an Effective Tool to Explore the Variety of Cocrystal Systems: Caffeine/dicarboxylic Acid Cocrystals. *Cryst. Eng. Commun.* **2014**, *16*, 9603–9611.

(10) Trask, A. V.; Jones, W. Crystal Engineering of Organic Cocrystals by the Solid-State Grinding Approach. *Topics in Current Chemistry*. 2005, pp 41–70.

(11) James, S. L.; Adams, C. J.; Bolm, C.; Braga, D.; Collier, P.; Friscic, T.; Grepioni, F.; Harris, K. D. M.; Hyett, G.; Jones, W.; Krebs, A.; Mack, J.; Maini, L.; Orpen, A. G.; Parkin, I. P.; Shearouse, W. C.; Steed, J. W.; Waddell, D. C.; Friščić, T.; Grepioni, F.; Harris, K. D. M.; Hyett, G.; Jones, W.; Krebs, A.; Mack, J.; Maini, L.; Orpen, A. G.; Parkin, I. P.; Shearouse, W. C.; Steed, J. W.; Waddell, D. C. Mechanochemistry: Opportunities for New and Cleaner Synthesis. *Chem. Soc. Rev.* **2012**, *41* (1), 413–447.

(12) Delori, A.; Friscic, T.; Jones, W.; Friščić, T.; Jones, W. The Role of Mechanochemistry and Supramolecular Design in the Development of Pharmaceutical Materials. *CrystEngComm* **2012**, *14* (7), 2350–2362.

(13) Jones, W.; Eddleston, M. D. Introductory Lecture: Mechanochemistry, a Versatile Synthesis Strategy for New Materials. *Faraday Discuss.* **2014**, *170* (0), 9–34.

(14) Boldyrev, V. V. Mechanochemistry and Mechanical Activation of Solids. *Russ. Chem. Rev.* **2006**, *75* (3), 177–189.

(15) Braga, D.; Grepioni, F. Solventless Reactions: Reactions between or within Molecular Crystals. *Angew. Chemie, Int. Ed.* **2004**, *43* (31), 4002–4011.

(16) Shan, N.; Toda, F.; Jones, W. Mechanochemistry and Co-Crystal Formation: Effect of Solvent on Reaction Kinetics. *Chem. Commun.* **2002**, No. 20, 2372–2373.

(17) Trask, A. V; Motherwell, W. D. S.; Jones, W. Solvent-Drop Grinding: Green Polymorph Control of Cocrystallisation. *Chem. Commun.* **2004**, No. 7, 890–891.
(18) FriŠčić, T.; Fabian, L.; Burley, J. C.; Jones, W.; Motherwell, W. D. S. Exploring Cocrystal-Cocrystal Reactivity via Liquid-Assisted Grinding: Assembling of Racemic and Dismantling of Enantiomeric Cocrystals . *Chem. Commun.* **2006**, *28* (48), 5009–5011.
(19) FriŠčić, T.; Trask, A. V; Jones, W.; Motherwell, W. D. S. Screening for Inclusion Compounds and Systematic Construction of Three-Component Solids by Liquid-Assisted Grinding. *Angew. Chemie* **2006**, *118* (45), 7708–7712.
(20) FriŠčić, T.; Childs, S. L.; Rizvi, S. A. A.; Jones, W. The Role of Solvent in Mechanochemical and Sonochemical Cocrystal Formation: A Solubility-Based Approach for Predicting Cocrystallisationoutcome. *Cryst. Growth Des.* **2009**, *11* (3), 418–426.
(21) Yamamoto, K.; Tsutsumi, S.; Ikeda, Y. Establishment of Cocrystal Cocktail Grinding Method for Rational Screening of Pharmaceutical Cocrystals. *Int. J. Pharm.* **2012**, *437* (1-2), 162–171.
(22) Shevchenko, A.; Miroshnyk, I.; Pietilä, L.-O.; Haarala, J.; Salmia, J.; Sinervo, K.; Mirza, S.; van Veen, B.; Kolehmainen, E.; Yliruusi, J. Diversity in Itraconazole Cocrystals with Aliphatic Dicarboxylic Acids of Varying Chain Length . *Cryst. Growth Des.* **2013**, *13* (11), 4877–4884.
(23) Lin, Y.; Yang, H.; Yang, C.; Wang, J. Preparation, Characterization, and Evaluation of Dipfluzine–Benzoic Acid Co-Crystals with Improved Physicochemical Properties. *Pharm. Res.* **2013**, 1–13.
(24) Sowa, M.; Ślepokura, K.; Matczak-Jon, E. A 1:1 Pharmaceutical Cocrystal of Myricetin in Combination with Uncommon Piracetam Conformer: X-Ray Single Crystal Analysis and Mechanochemical Synthesis. *J. Mol. Struct.* **2014**, *1058*, 114–121.
(25) Madusanka, N.; Eddleston, M. D.; Arhangelskis, M.; Jones, W. Polymorphs, Hydrates and Solvates of a Co-Crystal Ofcaffeine with Anthranilic Acid. *Cryst. Eng.* **2014**, *70* (1), 72–80.
(26) FriŠčić, T.; Jones, W. Cocrystal Architecture and Properties: Design and Building of Chiral and Racemic Structures by Solid–solid Reactions. *Faraday Discuss.* **2007**, *136*, 167–178.
(27) Medina, C.; Daurio, D.; Nagapudi, K.; Alvarez-Núñez, F. Manufacture of Pharmaceutical Co-Crystals Using Twin Screw Extrusion: A Solvent-Less and Scalable Process. *J. Pharm. Sci.* **2010**, *99* (4), 1693–1696.
(28) Dhumal, R.; Kelly, A.; York, P.; Coates, P.; Paradkar, A. Cocrystalization and Simultaneous Agglomeration Using Hot Melt Extrusion. *Pharm. Res.* **2010**, *27* (12), 2725–2733.
(29) Daurio, D.; Medina, C.; Saw, R.; Nagapudi, K.; Alvarez-Núñez, F. Application of Twin Screw Extrusion in the Manufacture of Cocrystals, Part I: Four Case Studies. *Pharmaceutics* **2011**, *3*, 582–600.
(30) Kelly, A. L.; Gough, T.; Dhumal, R. S.; Halsey, S. A.; Paradkar, A. Monitoring Ibuprofen–nicotinamide Cocrystal Formation during Solvent Free Continuous Cocrystallization (SFCC) Using near Infrared Spectroscopy as a PAT Tool. *Int. J. Pharm.* **2012**, *426* (1–2), 15–20.
(31) Kulkarni, C.; Wood, C.; Kelly, A. L.; Gough, T.; Blagden, N.; Paradkar, A. Stoichiometric Control of Co-Crystal Formation by Solvent Free Continuous

Co-Crystallization (SFCC). *Cryst. Growth Des.* **2015**, *15* (12), 5648–5651.
(32) Remenar, J. F.; Peterson, M. L.; Stephens, P. W.; Zhang, Z.; Zimenkov, Y.; Hickey, M. B. Celecoxib:Nicotinamide Dissociation: Using Excipients To Capture the Cocrystal's Potential. *Mol. Pharm.* **2007**, *4* (3), 386–400.
(33) Etter, M. C.; Reutzel, S. M.; Choo, C. G. Self-Organization of Adenine and Thymine in the Solid State. *J. Am. Chem. Soc.* **1993**, *115* (10), 4411–4412.
(34) Grzesiak, A. L.; Uribe, F. J.; Ockwig, N. W.; Yaghi, O. M.; Matzger, A. J. Polymer-Induced Heteronucleation for the Discovery of New Extended Solids. *Angew. Chemie - Int. Ed.* **2006**, *45* (16), 2553–2556.
(35) Hasa, D.; Schneider Rauber, G.; Voinovich, D.; Jones, W. Cocrystal Formation through Mechanochemistry: From Neat and Liquid-Assisted Grinding to Polymer-Assisted Grinding. *Angew. Chemie* **2015**, *127* (25), 7479–7483.
(36) Qiu, S.; Li, M. Effects of Coformers on Phase Transformation and Release Profiles of Carbamazepine Cocrystals in Hydroxypropyl Methylcellulose Based Matrix Tablets. *Int. J. Pharm.* **2015**, *479* (1), 118–128.
(37) Yazdanian, M.; Briggs, K.; Jankovsky, C.; Hawi, A. The "high Solubility" definition of the Current FDA Guidance on Biopharmaceutical Classification System May Be Too Strict for Acidic Drugs. *Pharm. Res.* **2004**, *21* (2), 293–299.
(38) Alshahateet, S. F. Synthesis and Supramolecularity of Hydrogen-Bonded Cocrystals of Pharmaceutical Model Rac-Ibuprofen with Pyridine Derivatives. *Mol. Cryst. Liq. Cryst.* **2010**, *533* (1), 152–161.
(39) Aakeröy, C. B.; Beatty, A. M.; Helfrich, B. A. A High-Yielding Supramolecular Reaction. *J. Am. Chem. Soc.* **2002**, *124* (48), 14425–14432.
(40) Aakeröy, C. B.; Beatty, A. M.; Helfrich, B. A.; Nieuwenhuyzen, M. Do Polymorphic Compounds Make Good Cocrystallizing Agents? A Structural Case Study That Demonstrates the Importance of Synthon Flexibility. *Cryst. Growth Des.* **2003**, *3* (2), 159–165.
(41) Bathori, N. B.; Lemmerer, A.; Venter, G. A.; Bourne, S. A.; Caira, M. R. Pharmaceutical Co-Crystals with Isonicotinamide-Vitamin B3, Clofibric Acid, and Diclofenac-and Two Isonicotinamide Hydrates. *Cryst. Growth Des.* **2011**, *11*, 75–87.
(42) Thommes, M.; Ely, D. R.; Carvajal, M. T.; Pinal, R. Improvement of the Dissolution Rate of Poorly Soluble Drugs by Solid Crystal Suspensions. *Mol. Pharm.* **2011**, *8*, 727–735.
(43) Padrela, L.; de Azevedo, E. G.; Velaga, S. P. Powder X-Ray Diffraction Method for the Quantification of Cocrystals in the Crystallization Mixture . *Drug Dev. Ind. Pharm.* **2012**, *38* (8), 923–929.
(44) Guidelines, I. C. H. Internation Conference on Harmonization (ICH) Harmonized Tripartite Guideline, Note for Guidance on Validation of Analytical Procedures: Methodology. ICH Steering Committee 1996.
(45) Leiserowits, L. Molecular Packing Modes. Carboxylic Acids. *Acta Crystallogr. Sect. B Struct. Crystallogr. Cryst. Chem.* **1976**, *32*, 775–802.
(46) Desiraju, G. R. *Crystal Engineering: The Design of Organic Solids*; Elsevier: Amsterdam, 1989.
(47) Steiner, T. The Hydrogen Bond in the Solid State. *Angew. Chemie Int. Ed.* **2002**, *41* (1), 48–76.
(48) Oswald, I. D. H.; Motherwell, W. D. S.; Parsons, S. A 1 : 2 Co-Crystal of Isonicotinamide and Propionic Acid . *Acta Crystallogr. Sect. E Struct. Reports Online* **2004**, *60* (12).

(49) Vueba, M. L.; Pina, M. E.; Batista De Carvalho, L. A. E. Conformational Stability of Ibuprofen: Assessed by DFT Calculations and Optical Vibrational Spectroscopy. *J. Pharm. Sci.* **2008**, *97* (2), 845–859.
(50) Silverstein, M.; Bassler, G. C.; Morrill, T. C. Spectrometric Identification of Organic Compounds ; J. Wiley & Son Inc.: New York, 1991; Vol. 5th, pp 117–123.
(51) Logansen, A. V; Kurkchi, G. A.; Dement'eva, L. A. Infrared Spectra of Primary Amides in the vNH Range. *J. Struct. Chem.* **1977**, *18* (4), 589–595.
(52) Sharma, B. K. Infrared Spectroscopy. In *Spectroscopy*; GOEL Publishing House: Meerut Delhi, 2007; Vol. 20th, pp 309–311.
(53) Filho, O. T.; Pinheiro, J. C.; da Costa, E. B.; Kondo, R. T.; de Souza, R. A.; Nogueira, V. M.; Mauro, A. E. Theoretical and Experimental Study of the Infrared Spectrum of Isonicotinamide. *J. Mol. Struct. THEOCHEM* **2006**, *763*, 175–179.
(54) Socrates, G. *Infrared and Raman Characteristic Group Frequencies*; 2004.
(55) Ramalingam, S.; Periandy, S.; Govindarajan, M.; Mohan, S. FT-IR and FT-Raman Vibrational Spectra and Molecular Structure Investigation of Nicotinamide: A Combined Experimental and Theoretical Study. *Spectrochim. Acta. A. Mol. Biomol. Spectrosc.* **2010**, *75* (5), 1552–1558.
(56) Tothadi, S.; Desiraju, G. R. Unusual Co-Crystal of Isonicotinamide: The Structural Landscape in Crystal Engineering. *Philos. Trans. R. Soc. A Math. Phys. Eng. Sci.* **2012**, *370*, 2900–2915.
(57) Steiner, T.; Desiraju, G. R. *The Weak Hydrogen Bond in Structural Chemistry and Biology*; Oxford University Press: New York, 1999.
(58) Doherty, C.; York, P. Fresemide Crystal Forms; Solid State and Physicochemical Analyses. *Int. J. Pharm.* **1988**, *47* (1-3), 141–155.
(59) Romero, A. J.; Savastano, L.; Rhodes, C. T. Monitoring Crystal Modifications in Systems Containing Ibuprofen. *Int. J. Pharm.* **1993**, *99* (2–3), 125–134.
(60) Lu, E.; Rodriguez-Hornedo, N.; Suryanarayanan, R. A Rapid Thermal Method for Cocrystal Screening. *Cryst. Eng. Commun.* **2008**, *10*, 665–668.
(61) FriŠčić, T.; Jones, W. Benefits of Cocrystallisation in Pharmaceutical Materials Science: An Update. *J. Pharm. Pharmacol.* **2010**, *62*, 1547–1559.
(62) Schultheiss, N.; Newman, A. W. Pharmaceutical Cocrystals and Their Physicochemical Properties. *Cryst. Growth Des.* **2009**, *9* (6), 2950–2967.
(63) Almarsson, Ö.; Peterson, M. L.; Zaworotko, M. J. The A to Z of Pharmaceutical Cocrystals: A Decade of Fast Moving New Science and Patents. *Pharm. Pat. Anal.* **2012**, *1* (3), 313–327.
(64) Alhalaweh, A.; Velaga, S. P. Formation of Cocrystals from Stoichiometric Solutions of Incongruently Saturating Systems by Spray Drying. *Cryst. Growth Des.* **2010**, *10* (8), 3302–3305.
(65) Alhalaweh, A.; Kaialy, W.; Buckton, G.; Gill, H.; Nokhodchi, A.; Velaga, S. P. Theophylline Cocrystals Prepared by Spray Drying: Physicochemical Properties and Aerosolization Performance. *AAPS PharmSciTech* **2013**, *14* (1), 265–276.
(66) Gryczke, A.; Schminke, S.; Maniruzzaman, M.; Beck, J.; Douroumis, D. Development and Evaluation of Orally Disintegrating Tablets (ODTs) Containing Ibuprofen Granules Prepared by Hot Melt Extrusion. *Colloids Surfaces B Biointerfaces* **2011**, *86* (2), 275–284.
(67) Quentiros, D. A.; Allemandi, D. A.; Manzo, R. H. Equilibrium and Release Properties of Aqueous Dispersions of Non-Steroidal Anti-Inflammatory Drugs

Complexed with Polyelectrolyte Eudragit E 100. *Sci. Pharm.* **2012**, *80* (2), 487–496.
(68) Onoue, S.; Kojo, Y.; Aoki, Y.; Kawabata, Y.; Yamauchi, Y.; Yamada, S. Physical Chemical and Pharmacokinetic Characterization of Amorphous Solid Dispersion of Tranilast with Enhanced Solubility in Gastric Fluid and Improved Oral Bioavailability. *Drug Metab. Pharmacokinet. Adv. Publ.* **2012**.
(69) Acton, Q. A. *Sugar Alcohols—Advances in Research and Application*; ScholarlyEditions: Atlanta, Geogia, 2013; Vol. 2013.
(70) Aakeröy, C. B.; Grommet, A. B.; Desper, J. Co-Crystal Screening of Diclofenac. *Pharmaceutics* **2011**, *3* (3), 601–614.
(71) Alatas, F.; Soewandhi, S. N.; Sasongko, L.; Ismunandar; Uekusa, H. Cocrystal Formation between Didanosine and Two Aromatic Acids. *Int. J. Pharm. Pharm. Sci.* **2013**, *5* (Suppl 3), 275–280.
(72) Allen, L. V. J.; Yanchick, V. A.; Maness, D. D. Dissolution Rates of Corticosteroids Utilizing Sugar Glass Dispersions . *J. Pharm. Sci.* **1977**, *66* (4), 494–497.
(73) Leuner, C.; Dressman, J. Improving Drug Solubility for Oral Delivery Using Solid Dispersions. *Eur. J. Pharm. Biopharm.* **2000**, *50* (1), 47–60.
(74) Perissutti, B.; Newton, J. M.; Podczeck, F.; Rubessa, F. Preparation of Extruded Carbamazepine and PEG 4000 as a Potential Rapid Release Dosage Form. *Eur. J. Pharm. Biopharm.* **2002**, *53* (1), 125–132.
(75) Li, C.; Li, C.; Le, Y.; Chen, J.-F. Formation of Bicalutamide Nanodispersion for Dissolution Rate Enhancement. *Int. J. Pharm.* **2011**, *404* (1–2), 257–263.
(76) Eddleston, M. D.; Patel, B.; Day, G. M.; Jones, W. Cocrystallization by Freeze-Drying: Preparation of Novel Multicomponent Crystal Forms. *Cryst. Growth Des.* **2013**, *13* (10), 4599–4606.
(77) Rumondor, A. C. F.; Stanford, L. A.; Taylor, L. S. Effects of Polymer Type and Storage Relative Humidity on the Kinetics of Felodipine Crystallization from Amorphous Solid Dispersions. *Pharm. Res.* **2009**, *26* (12), 2599–2606.
(78) Stevens, M. J.; Covas, J. A. *Extruder Principles and Operation*; Chapman & Hall: 2-6 Boundary Row, London SE1 8HN, UK, 1995; Vol. Second edi.
(79) Dreiblatt, A. Process Design. In *Pharmaceutica Extrusion Technology*; Ghebre-Sellassie, I., Martin, C., Eds.; Marcel Dekker, Inc.: New York, 2003; pp 153–169.
(80) Thiele, W. Twin-Screw Extrusion and Screw Design. In *Pharmaceutical Extrusion Technology*; Ghebre-Sellassie, I., Martin, C., Eds.; Marcel Dekker, Inc: New York, 2003; pp 69–98.
(81) Douroumis, D. *Hot-Melt Extrusion: Pharmaceutical Extrusions*; John Wiley & Sons Ltd: West Sussex, UK, 2012.
(82) Reitz, E.; Podhaisky, H.; Ely, D.; Thommes, M. Residence Time Modeling of Hot Melt Extrusion Processes. *Eur. J. Pharm. Biopharm.* **2013**, *85* (3 PART B), 1200–1205.